PSBO SAMPLES A COMPLEX CONFORMATIONAL LANDSCAPE WHICH IS REGULATED BY PHOTOSYSTEM II

A Dissertation
Presented to
The Academic Faculty

by

Jiayuan He

In Partial Fulfillment
of the Requirements for the Degree
Master of Science in the
School of Chemistry & Biochemistry

Georgia Institute of Technology
August 2020

PSBO SAMPLES A COMPLEX CONFORMATIONAL LANDSCAPE

WHICH IS REGULATED BY PHOTOSYSTEM II

Approved by:

Dr. Bridgette Barry, Advisor
School of Chemistry and Biochemistry
Georgia Institute of Technology

Dr. Facundo Fernandez
School of Chemistry and Biochemistry
Georgia Institute of Technology

Dr. Ronghu Wu
School of Chemistry and Biochemistry
Georgia Institute of Technology

Date Approved: July 7th, 2020

ACKNOWLEDGEMENTS

First and foremost, I would like to thank my principle investigator Dr. Bridgette Barry. I do appreciate that she gave the chance to join her lab and get the opportunities to get the professional training as a biochemistry scientist. I would like to thank Dr. Udita Bramachari, Dr. Tyler McCaslin, Dr. Zhanjun Guo and Dr. Jiafeng Geng for their support and guidance to my graduate student life and research. I would also like to thank all current members in Barry group for the exciting discussion of science. I am grateful to my committee members, Dr. Facundo Fernandez and Dr. Ronghu Wu. I would also like to acknowledge Dr. David Smalley in EBB MS facility and IBB core facility for their collaboration and support throughout the course of my research. I sincerely appreciate all the assistance and instructions from the department coordinator, Dr. Johnson Kenyetta and the department chair, Dr. M.G. Finn. Finally, I would like to thank my roommate, all my friends, and my family in China. All of you are important parts of my four-year life in Georgia Tech.

TABLE OF CONTENTS

LIST OF TABLES

LIST OF FIGURES

LIST OF SYMBOLS AND ABBREVIATIONS

PSII	Photosystem II
OEC	Oxygen evolving complex
LHC	Light harvesting complex
OTG	Ocytlthioglucoside
CD	Circular dichroism
UVRR spectroscopy	Ultra-violet resonance Raman spectroscopy
FPLC	Fast protein liquid chromatography
SDS-PAGE	Sodium dodecyl sulfate polyacrylamide gel electrophoresis
WT	Wild type
CNF	Cyanophenylalanine
XFEL	X-Ray Free-Electron Laser
Cryo-EM	Cryogenic electron microscopy
7AW	7-azatryptophan
FT-IR	Fourier-transfer infrared spectroscopy
ENDOR	Electron-nuclear double resonance
EPR spectroscopy	Electron paramagnetic resonance
EXAFS	Extended X-Ray Absorption Fine Structure

SUMMARY

The maintenance of aerobic heterotrophic life relies on the photosynthetic oxygen production in the PSII reaction center. This reaction is intrinsically important in biological chemistry. Moreover, the efficiency of transferring solar energy to chemical energy makes PSII an excellent candidate for modeling the design and development of sustainable and biomimetic forms of artificial energy. PSII is a multisubunit transmembrane complex. It consists of several membrane-spanning helices and three main extrinsic subunits. PsbO is proposed to be an IDP when isolated free in solution. Its secondary structure showed significant change after bound to PSII, which is referred as templating effect. MS, CD and UVRR are used in my study to locate the residues that respond to the regulation of PSII. The current work provides new structural/conformational information concerning an indispensable part of the photosynthetic oxygen production reaction, PsbO, an extrinsic subunit of PSII.

CHAPTER 1. INTRODUCTION

1.1 Photosystem II

Table 1 – PSII structure summary

PDB ID	Source Organism	Resolution (Å)	Method
4PJ0	*Thermosynechococcus elongatus*	2.44	X-ray diffraction
5KAF		3.00	XFEL
5B66	*Thermosynechococcus vulcanus*	1.85	X-ray diffraction
6JLJ		2.15	XFEL
1FE1	*Synechococcus elongatus*	3.8	X-ray diffraction
3JCU	*Spinacia oleracea*	3.2	Cryo-EM
5MDX	*Arabidopsis thaliana*	5.3	Cryo-EM
6KAC	*Chlamydomonas reinhardtii*	2.7	Cryo-EM
4YUU	*Cyanidium caldarium*	2.77	X-ray diffraction
6J3Y	*Chaetoceros gracilis*	3.3	Cryo-EM

Photosynthesis consists of light reaction and dark reaction. The light reaction oxidizes water to molecular oxygen. The dark reaction converses carbon dioxide to carbohydrates. Photosynthesis is the conversion from solar energy to chemical energy. It sustains aerobic and heterophilic life on earth. Photosynthetic machinery is housed in the chloroplast. The first part of photosynthesis is the light reaction at photosystem (PSII). PSII is a very complex protein, consisting of several membrane spanning helix and three main extrinsic subunits.[1-3] As is shown in Figure 1A, four important intrinsic subunits, D1, D2, CP43 and CP47 are colored. They are in contact with most of the redox-active cofactors. There is a light-induced electron transfer pathway in the reaction center. The dimeric chlorophyll (Chl) donor, P_{680}, accessory chlorophyll molecules, quinone acceptors and YZ (D1-Tyr-161) all play a role in this pathway.[4-5] PSII exists in plants[3, 6], algae[7-9] and cyanobacteria[10-14]. The PSII structures from various organisms are summarized in table 1.

An extensive set of site-directed mutagenesis[15-20] and labelling[21-26] experiments have been performed to study PSII structure and dynamic.

1.2 Oxygen evolving complex

Photoinduced oxidation of water happens at a Mn_4CaO_5 cluster which is organized in a distorted-chair form. (Figure 1B) The metal cluster also named as oxygen-evolving complex (OEC). In the metal cluster, an external Mn is attached to a Mn_3CaO_4 cubane by two μ-oxo O4 and O5 atoms.[1-2] The OEC is surrounded by a node of five water channels[1] that play critical role in proton release, balancing net charge of the OEC and inlet of substrate water.[27-28] Oxygen generated from the cluster in the period of four flashes with the liberation of proton.[29] The cycle of OEC sequential oxidation is modeled as S_n states. *n* refers to the number of oxidizing equivalents stored on the catalytic site. Subsequent flashes allow the evolution of OEC to higher S states and higher oxidation states. Dioxygen is generated in the final step of the S-state cycle ($S_3 \rightarrow S_4 \rightarrow S_1$).[29] Many progress along with controversy occurred on the way to determine the structure of OEC in specific catalytic states with higher resolution.[12-13, 30-35] For example, in 2015, when a radiation-damage-free Mn_4CaO_5 cluster was published[2], it was assumed to be in S_1 state. However, this assumption disagreed with ENDOR, EPR and EXAFS data in S_1 state published earlier.[28, 36-37] Later in the same year, the structure was suggested that it probably was a combination of the reduced S_0 and S_1 state.[38] A structure change, dislocation of W665 in the O4 channel during the process of S_i state, was attributed to a proton release through the O4 channel.[2, 35] However, other groups argued that W665 works as the source of the O6 atom involved in O=O bond formation.[39-40] A high-resolution S_2 state structure may be

necessary to clarify structural changes leading to or from this state. Due to the limited resolution of the S_3-state structure, the dioxygen formation mechanism was undetermined. There were several candidates for this reaction mechanism, including an oxyl/oxo radical coupling mechanism[41], a nucleophilic attack reaction mechanism[42] or a peroxide intermediate mechanism[43]. In 2019, Suga et al. revealed that the O=O bond formation happens through the oxyl/oxo coupling mechanism.[13] Two water substrate were believed to be involved in $S_4 \rightarrow S_0$, [44] while one of the water molecule was suggested to join the reaction during the $S_2 \rightarrow S_3$ transition.[32] There were at least seven candidates for the two substrate water molecules.[45] Experiments showed that two substrates exchange at different rates [water slow (W_S) and water fast (W_f)].[46-47] O5 of the μ-oxo bridges represented a hydroxo in the state, which can explain the enhanced W_S in the S_0 state.[48] The second water substrate, W_f, cannot be determined yet. [45]

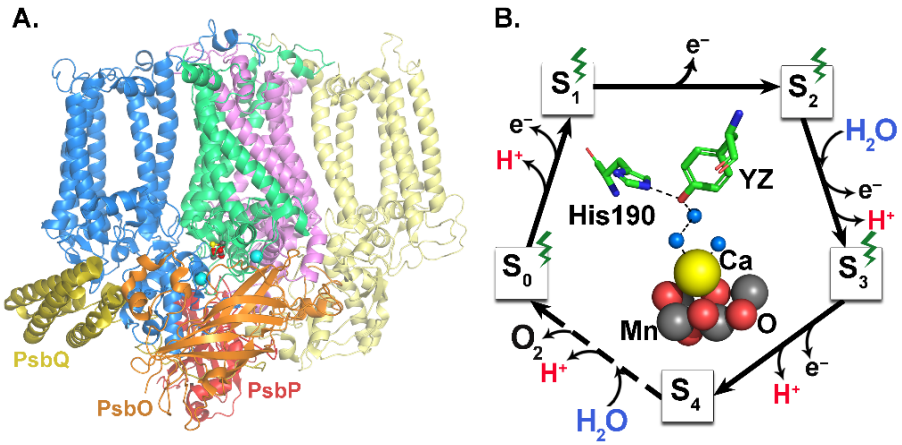

Figure 1 – Spinach PSII structure and photosynthetic water oxidation S-state cycle. (A) Spinach PSII structure (PDB ID: 3JCU[49]) including four important intrinsic subunits (D1 - green, D2 – magenta, CP43 - marine, CP47 - yellow) and three main extrinsic subunits (PsbO – orange, PsbP - red, PsbQ - olive). (B) S-state cycle of water oxidation. (B, Inset) The OEC (Ca – yellow, Mn – grey, O - red) in cyanobacterial PSII, in which bound water molecules (small blue spheres) are assigned (PDB: 4UB6[50]).

1.3 PsbO

PsbO consists of 231-257 amino acids. It is expressed in all oxygenic photosynthetic organisms.[51] PsbO sequence is 60-80% conservative among high plants and algae. Among lower plants and cyanobacteria, PsbO sequence conserves around 40%.[52] A set of site-directed mutagenesis study on important PsbO residues have been operated to study their functional meaning.[53-59] Stoichiometry of PsbO-PSII binding can be different among species. Cyanobacteria PSII has one copy of PsbO bond.[52] Some plants only have one copy of PsbO per reaction center in PSII in plants, such as rice (*Oryza sativa*) and pea (*Pisum sativum*), while others may have to isoforms of PsbO, like potato (*Solanum tuberosum*) and Arabidopsis (*Arabidopsis thaliana*).[60] Differences in sequence and function between two isoforms, PsbO-1 and PsbO-2, have been wildly studied. Both PsbO isoforms are active in photosynthesis, though their functions hold differences.[61-66]

PsbO along with other two extrinsic subunits, PsbP and PsbQ are necessary to maintain the high steady-state oxygen evolution rates.[52, 67-69] They PsbP and PsbQ are proposed to manipulate the retention of the calcium and chloride ions for OEC.[70] Chloride can function as a PSII activity regulator. Mutagenesis studies in cyanobacteria PSII supported this idea.[71-72] PsbO also plays similar role and it accelerates the water-splitting reaction.[73] The surface of PsbO hosts an wide web of carboxylate/water hydrogen-bonding network.[74] Site-directed mutagenesis has been applied to propose the proton exit pathway.[75-78] After protons are liberated from the OEC, they transfer through hydrogen bonding network, pass through PsbO and reaches the lumen side.[50, 79-80] (Figure 2) Molecular dynamic simulations have modeled many active water/carboxylate dimers on PsbO.[81-82] For example, a carboxylate cluster, D222/D223/D224 in cyanobacteria PsbO is

suggested to be critical structural and energetic determinants of a proton-transfer network. The D224 residue is also suggested to be part of the hydrogen bonding network that facilitate the docking of PsbO to PSII.[74] Water molecules involved in hydrogen bonding has lower mobility than that of bulk water. The sacrifice of mobility may be helpful to PsbO binding to PSII since water molecules are known to be able to mediate favorable protein/protein interactions and/or enhance electrostatic interactions between proteins to ease protein binding.[83] Though PsbO structure when it is bound to PSII has been defined, PsbO is proposed to be intrinsically disordered when it is free in aqueous solution[84] and its structure/conformation is undetermined yet.[6, 85-86]

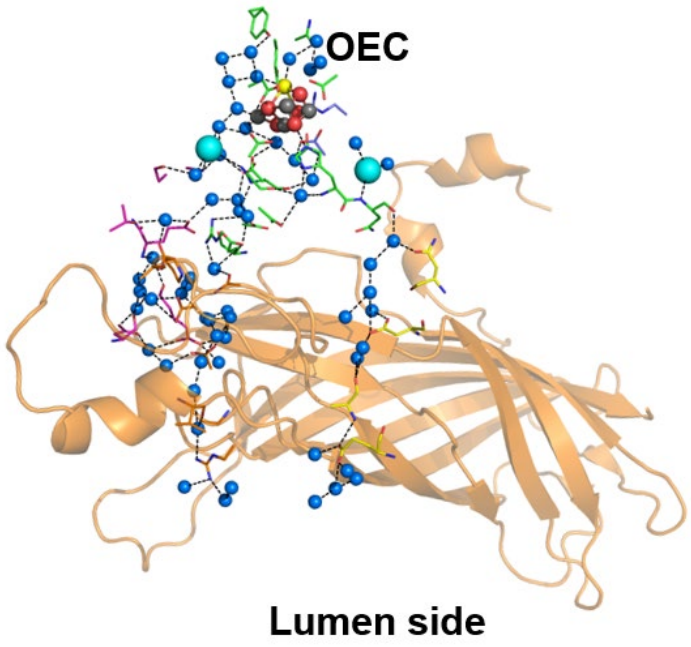

Figure 2 - Putative proton transfer pathways from the OEC to the lumen in the cyanobacterial PSII structure (PDB 4UB6). Residues that are proposed to be involved in the proton exit pathway are shown in stick. Water – small blue sphere; chloride – cyan sphere.

1.4 Intrinsically disordered protein

Intrinsically disordered proteins (IDPs) are proteins retaining it biological activity, though they lack ordered structure and hold a broad ensemble of dynamic conformations.[87-88] In addition, the sequences of IDPs usually have low complexity and high ratio of charged to hydrophobic amino acids[87], which results in high "PONDR (Predictor of Naturally Disordered Regions)" score[89]. PONDR is a neutral network predictor which is utilized to predict intrinsic order or disorder. PONDR score larger than 0.5 indicates disordered structure. Smaller than 0.5 indicates ordered structure. Factors including amino acid composition, sequence complexity, hydrophobicity, charge and flexibility, etc, are attributed to the PONDR score.[90] IDPs are involved in a significant number of biological processes and play important roles. The transitions between disordered- and ordered-status allows IDPs to achieve highly specific protein-protein interactions via a coupled folding, recognition and binding mechanism.[91] Human disease is a region where IDPs have a wide range of implications.[92] PsbO is hypothesized to be an IDP for several properties. For example, PsbO has a low pI. Its size gets exaggerated on SDS-PAGE and size exclusion chromatography. It has a large amount of random coils and turns.[84, 93]

1.5 Unnatural amino acids

1.5.1 Cyanophenylalanine (CNF)

CNF is a popular probe used in protein conformation and dynamics study.[94] It is a good fluorescence probe due to several reasons.[95-96] First, CNF can be selectively excited at 240 nm. Second, CNF is a sensitive fluorescence probe. Its fluorescence quantum yield (0.11) is around five times of phenylalanine (0.022). Third, it is easy to accommodate into protein in various environment, with minimally interruption to protein structure. Fourth,

its fluorescence responds to the hydrogen bonding condition of the C=N group. In addition, CNF is a good vibrational spectroscopic. [97-98] Its peak frequency and linewidth are sensitive to the change in the local electrostatistics. The absorbance of CNF is maximized ~230 nm so the application of UV probe at 229 nm or 244 nm on protein sample with CNF incorporation can detect vibrational spectrum with high UV resonance signal. Another advantage of CNF as Raman probe is that its wavenumber falls in 2150-2250 cm^{-1}, no overlapping with any of the common vibrational bands of proteins.[99-100] UV resonance Raman has been used to study conformational switching in PSII-inspired biomimetic peptides[101] and other moquette[102-103]. The method can be consulted and adjusted for the conformational study of the CNF incorporated PsbO.

1.5.2 7-azatryptophan (7AW)

7AW is a commercially available unnatural amino acid. It has been successfully incorporated into recombinant protein for structure and dynamics study.[104] 7AW has unique and pH-sensitive vibrational frequencies that make it a practical probe for light-induced proton transfer. 7AW has been successfully and noninvasively incorporated into PsbO as a substitution to W241 and it has been proved to be a nice tool for the definition of the internal proton pathway in PsbO.[67, 105] The reconstituted 7AW(241)PsbO-PSII did not exhibit significant change in oxygen evaluation activity or flash-dependent protein dynamics. The frequencies and intensity of the 7AW vibrational bands are sensitive to the light induced protonation that can be evaluated by UVRR[101, 106] and FT-IR[107] spectroscopy. Moreover, 7AW shows unique optical and fluorescent properties that are impacted by the protonation status of the azaindole group.[105]

1.6 UV Resonance Raman (UVRR) spectroscopy

UVRR spectroscopy uses ultraviolet laser as an excitation source to resonantly enhance the spectral contributions of aromatic amino acid residues in protein samples, such as tyrosine and tryptophan.[108] This method provides high resolution spectrum. Vibrational frequencies and intensities of reflect perturbation these aromatic residues. They are structural and environmental markers of protein samples. The spectrum indicates changes including hydrogen bonding, metal binding, redox state, protonation state, dielectric constant and etc.[106, 109] UVRR spectroscopy has been widely applied for protein conformational change and reaction dynamics study.[110-113] The additional microprobe jet flow technique is designed to prevent UV degradation of the analyte. At 244 nm or 229 nm, the second harmonic of a continuous wave Ar-ion laser lowers the fluorescence background and weakens the Raman scattering from water. The Raman microscope system achieves high signal collection efficiency with sufficient space for the jet flow cell.[108]

CHAPTER 2. MATERIALS AND METHODS

2.1 Photosystem II and PsbO sample preparation

2.1.1 PSII extraction

Two detergents, Triton X-100 (Sigma) and octylthioglucoside (OTG; Anatrace) were used to extract PSII-enriched thylakoid membranes from market spinach, as preciously described.[114-115] The PSII sample isolated by Triton X-100 is named as BBY-PSII, using the last name initial of the three scientists who established this methods. The PSII cores after both detergents' treatment is named as OTG-PSII. (Figure 3) The PSII samples were suspended in SMN-15 buffer, containing 0.40 M sucrose, 50 mM 2-(N-morpholino)-ethanesulfonic acid (MES)-NaOH, pH 6.0, and 15 mM NaCl, and stored at -70℃.

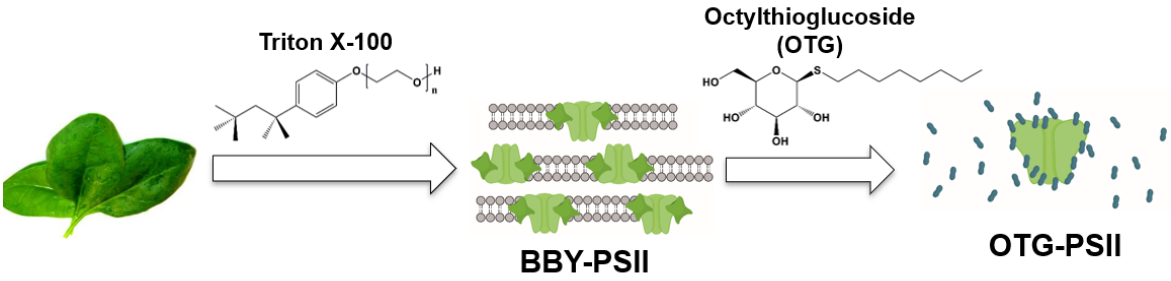

Figure 3 – PSII extraction by detergent solubilization from market spinach. Triton X-100 isolates PSII-enriched membranes fragments with intact LHC. OTG removes membranes and LHC, leaving PSII cores with extrinsic poly peptides.

2.1.2 Oxygen Evolution Assay

A Clark-type oxygen electrode was used to assay the oxygen evolution activity of the PSII samples. External electron acceptors, freshly prepared 1.0 mM potassium

ferricyanide ($K_3[Fe(CN)_6]$) and recrystallized 0.50 mM 2,6-dichlorobenzoquinone (DCBQ), were added. Measurements were performed at pH 6.0. The buffer contained 0.40 M sucrose, 50 mM MES-NaOH and 15 mM NaCl.

2.1.3 Native PsbO isolation

PSII samples were incubated with 2.0 M NaCl to remove PsbP and PsbQ. Samples are further incubated with 2.6 M urea/0.20 M NaCl[116] or 1.0 M $CaCl_2$[117] to isolate natively bound PsbO (native PsbO). Urea-washed PsbO (UW-PsbO) and $CaCl_2$-washed PsbO ($CaCl_2$-PsbO) are dialyzed and purified as described in literature.[117] The Amersham Biosciences AKTA Fast protein liquid chromatography (FPLC) system was used to do further purification. It was equipped with a Superose 12 HR 10/30 (Amersham Biosciences). The running buffer contains 100 mM NaCl and 20 mM sodium phosphate, pH 6.5. After loading 0.50 ml PsbO sample, the system was run with a constant flow of 0.50 ml/min, and fractionation was started after the UV absorption significantly increased. Samples are frozen and stored at -70 ℃.

2.1.4 R-V235A PsbO and WT-PsbO overexpression and isolation

E.coli BL21(DE3)/pLysS cells, containing the PsbO overexpression plasmid, were used for R-V235A PsbO overexpression and purification.[118-120] WT PsbO was generated by reversing the V235A mutation, using QuikChange II Site-Directed Mutagenesis Kit (Agilent Technology). The Met at the N terminal still exits. R-V235A PsbO and WT PsbO are respectively purified with method in previous paper.[67] Isolated PsbO were dialyzed into 50 mM MES-NaOH (pH 6.0) and 10 mM NaCl. Same FPLC system and experimental conditions were performed to collect fractions. Samples were frozen and stored at -70 ℃.

2.1.5 CNF site specific incorporation into PsbO

An evolved synthetase system and a TAG stop code were used to incorporated CNF into PsbO to substitute F40, F55, F155 and F217 (spinach PsbO numbering).[121-122] Mutagenesis was performed by using QuikChange II Site-Directed Mutagenesis Kit (Agilent Technology). The CNF-PsbO was purified from *E.coli* BL21(DE3) cells, containing the PsbO overexpression plasmid and the pDule-pCNF plasmid. The sequences of both plasmids were verified before the transformation. The selection media contained tetracycline and ampicillin. Methods for protein purification are included in previous literature.[67] Isolated PsbO were dialyzed into 5 mM 4-(2-hydroxyenthyl)-1-piperazineethanesulfonic acid (HEPES) (pH 7.5) and 15 mM NaCl. Samples were frozen and stored at -70℃.

2.1.6 PsbO reconstitution and templated PsbO sample preparation

Natively bound extrinsic subunits (PsbP/PsbQ and PsbO) are removed by incubation with 2.0 M NaCl and 2.6 M urea/0.20 M NaCl, respectively. R-V235A PsbO, WT PsbO or CNF-PsbO was reconstituted into urea-PSII (2.0 μM) in 0.40 M sucrose, 50 mM MES (pH 6.0), 60 mM NaCl and 20 mM $CaCl_2$, supplemented with 0.33 mg/ml bovine serum albumin (BSA, Fraction V). PsbO concentrations were 10 μM, corresponding to 5.0 mol of PsbO/mol of PSII reaction center. PsbO concentrations were estimated by an extinction coefficient, 16 $mM^{-1}cm^{-1}$ at 276 nm.[73] The rebinding reaction was carried out at room temperature in the dark for an hour. Non-specifically bound PsbO was removed by low spin centrifugation (12,000×*g*, 4°C, 10 min). Reconstituted PSII samples were resuspended in appropriate buffer. Urea-SDS-PAGE and western blot were used to analyze the

reconstituted PSII samples. Oxygen evolution assays[115] were performed to assess the efficiency of PsbO reconstitution. Samples were frozen and stored at -70℃. Reconstituted PSII samples are incubated with 2.6 M urea/0.20 M NaCl[116] to isolated the reconstituted PsbO. The pulled off PsbO is named as templated PsbO.

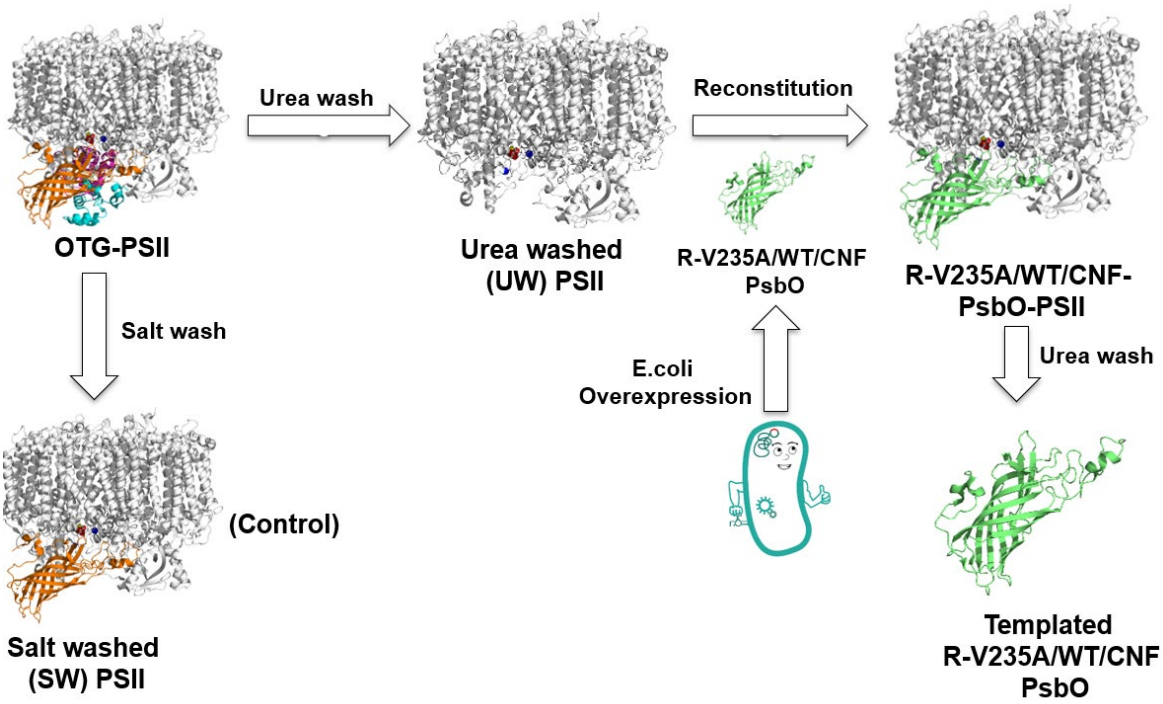

Figure 4 – R-V235A/WT/CNF-PsbO-PSII reconstitution scheme.

2.2 Photosystem II and PsbO sample characterization

2.2.1 SDS-PAGE and western blot analysis

SDS-PAGE analysis was performed as described previously.[123] Coomassie (Brilliant Blue R) was used to stain the gel. 1 μg of chlorophyll was loaded in each lane. Western blot analysis used a primary anti-PsbO rabbit antibody[124], a secondary anti-rabbit protein

A-alkaline phosphatase conjugate (Calbiochem) and a 5-bromo-4-chloro-3-indolyl phosphate/nitro blue tetrazolium (BCIP/NBT; Thermo Scientific) liquid substrate system.

2.2.2 UV-vis and fluorescence spectra

A Shimadzu UV-1700 spectrophotometer was used to record UV-Vis absorption spectra. Measurements were performed at room temperature in 1 cm quartz cuvettes. The scan settings were 0.5 nm interval and 1.0 nm slit width. For UV-Vis, the concentrations of protein were 2 μM and of CNF is 10 μM. A Shimadzu FR-5301PC fluorimeter in 1 cm methacrylate cuvettes was used to record fluorescence spectra. The slit widths were 3 nm excitation and 5 nm emission. For fluorescence, the concentrations of protein and CNF are 2 μM. Protein and CNF were in buffer containing 5 mM HEPES (pH 7.5) and 15 mM NaCl.

2.2.3 Mass spectral analysis

Mass spectra of WT PsbO and CNF PsbO were obtained at System Mass Spectrometry Facility in Engineered Biosystem Building of the Georgia Institute of Technology by Dr. David Smalley.

2.2.4 CD

CD spectra of 10 μM protein samples were collected from 250 nm to 200 nm in a 1.0 mm quartz cuvette using a JASCO J-815 CD Spectrometer, equipped with a Peltier-type cell. Twenty accumulations per scan were averaged in two independent measurements for each of the temperatures. Spectrum acquisition parameters: data pitch, 1.0 nm; scanning

speed, 20 nm/min; sample concentration, 10 μM; buffer, 10 mM KH_2PO_4, pH 6.0. A web server, BeStsel, was used to perform protein secondary structure analysis.[125-126]

2.2.5 UVRR spectroscopy

UVRR spectroscopy instrument set-up scheme is shown in Figure 5. UVRR spectra were acquired at 8 cm^{-1} resolution, with 3.8 mW 244 nm excitation probe beam, over 4 min exposure time and at room temperature. Information of instrument, data collection methods and data analysis have been reported in detail previously.[101, 108, 127] The experiments were performed with 45 μM protein samples and 20 μM CNF in 5 mM HEPES (pH 7.5) and 15 mM NaCl. At least two measurements are averaged to generate the spectra.

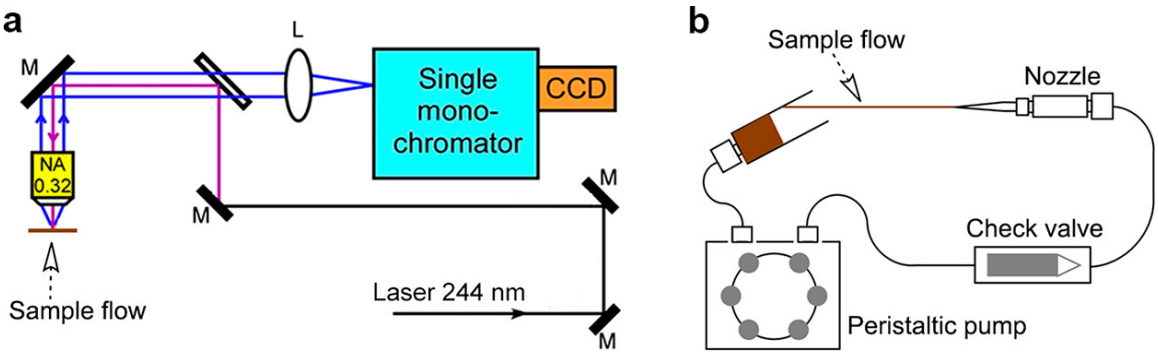

Figure 5 – UVRR spectroscopy instrument set-up scheme. Panel A, the 244 nm UV laser probe is guided to shoot vertically on the sample flow and the scattering is collected and finally reaches the CCD camera. Panel B, the protein samples were recirculated using a peristaltic pump through a nozzle (~ 120 μm inner diameter) to form a jet and the pump was plumbed with silicon tubing.[128]

CHAPTER 3. RESULTS

3.1 Site directed incorporation of cyanophenylalanine into WT PsbO

3.1.1 CNF incorporation into WT PsbO

Site specific incorporation of CNF into locations (F40, F57, F155 and F217) has been attempted. (Figure 6) These positions probed different structural domains of PsbO. F40 was in the random coil region domain distal from the proposed proton exit pathway. F155 was the in the loop region that participates in the proton exit pathway. F57 was located in the β-barrel, at the opposite side of F217. The CN incorporation at F217 was confirmed by MS.

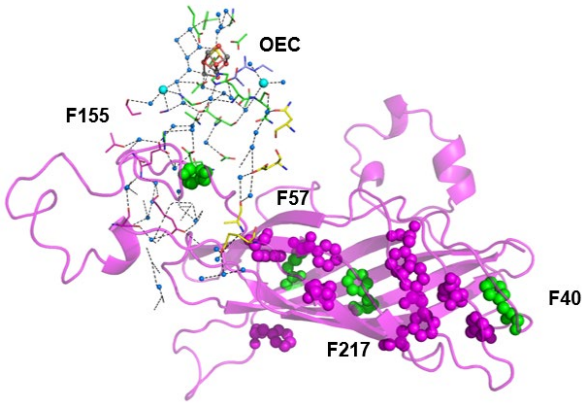

Figure 6 – Mapping CNF probes into the PSII proton transfer pathway (4UB6) from the OEC to the lumen, involving internal water (blue), amino acid side chains, and PsbO (PDB: 3JCU). All phenylalanines are shown in spheres. The phenylalanines, F155, F57, F217, and F40, mutated to CNF in initial experiments are shown in green. The unmutated phenylalanines are colored in magenta.

3.1.2 Fluorescence of CNF217 PsbO

The 310 nm peak was attributed to the intrinsic fluorescence of tyrosine in PsbO.[129] As shown in Figure 7A, upon exciting at 280 nm, CNF, WT PsbO and 1:1 mixture of (WT-

PsbO + CNF) had maximum emission at ~310 nm. The fluorescence of the CNF alone in aqueous solution was quenched due to the chloride in buffer.[95] In the case of CNF217-PsbO, an obvious red shift was detected, ~24 nm. There are three tyrosine residues within 15 Å of F217. The incorporation of nitrile group at residue 217 could interrupt the hydrogen bonding among aromatic side chains of residues. The shift in the fluorescence emission spectrum of PsbO reported the change of tyrosine-tyrosine interaction in PsbO and the interactions between other aromatic groups. (Figure 7B)

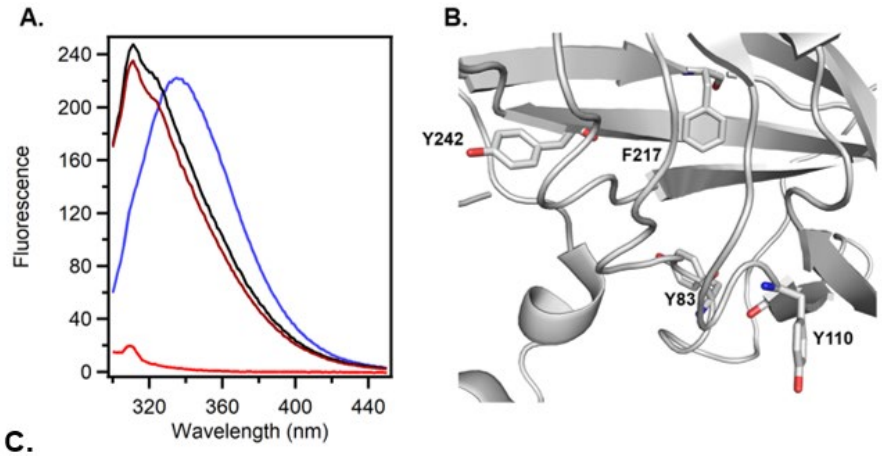

Figure 7 – PsbO intrinsic fluorescence. Panel A, fluorescence emission spectra of PsbO samples. 2 µM of each sample in 5 mM HEPES (pH 7.5) and 15 mM NaCl was excited at 280 nm. WT PsbO in black; CNF-red; 1:1 WT PsbO + CNF mixture; CNF217 PsbO in blue. CNF217 PsbO peaked at 334 nm. The other three samples peaked at 310 nm. CNF fluorescence was quenched. Panel B, PsbO zoom in view at F217. F217 and three tyrosines (Y83, Y110 and Y242) in 15 Å of F217 are shown in stick. Panel C, sequence of CNF217 PsbO. The Met at the N-terminal is count as number zero.

3.1.3 CNF217-PsbO-PSII reconstitution

The CNF217-PsbO-PSII reconstitution was confirmed by SDS-PAGE. (Figure 8). The PsbO band kept the same in OTG-PSII (lane 1) and SW-PSII sample (lane 2), while PsbP and PsbQ were lost after salt wash. After urea wash, the PsbO band became much lighter (lane 3). After the reconstitution of WT PsbO (lane 4) and CNF217 PsbO (lane 5), the band of PsbO got thicker compared with UW-PSII. Oxygen evolution assay results showed that the removal of PsbO led to the dramatically decrease of oxygen evolution activity. The reconstitution could restore the oxygen evolution rate in a level comparable to WT-PsbO-PSII. (Table 2) The steady-state oxygen evolution activity was in unit of μmol of O_2 (mg of Chl·h)$^{-1}$. The percent activity (+ Ca^{2+}) was relative to SW-PSII samples.

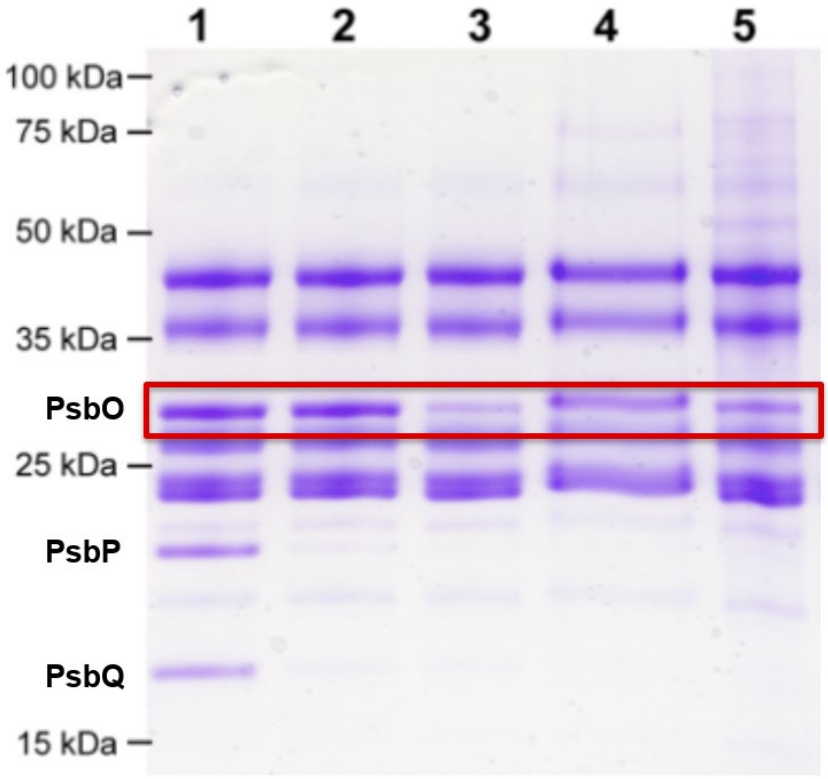

Figure 8 – CNF217-PsbO-PSII reconstitution SDS-PAGE gel. Lane 1, OTG-PSII; Lane 2, SW-PSII; Lane 3, UW-PSII; Lane 4, WT-PsbO-PSII; Lane 5, CNF217-PsbO-PSII. PsbO bands are boxed. PsbP and PsbQ are labelled near their bands.

Table 2 – Steady-state oxygen evolution activity of CNF217-PsbO-PSII samples

PSII sample	- Ca^{2+}	+ Ca^{2+}	% SW-PSII
OTG-PSII	1180 ± 50	1240 ± 40	
SW-PSII	660 ± 20	940 ± 20	100%
UW-PSII	390 ± 10	520 ± 10	55%
WT-PsbO-PSII	610 ± 40	790 ± 30	84%
CNF217-PsbO-PSII	550 ± 20	780 ± 20	83%

3.1.4 CNF40/57/155-PsbO-PSII reconstitution

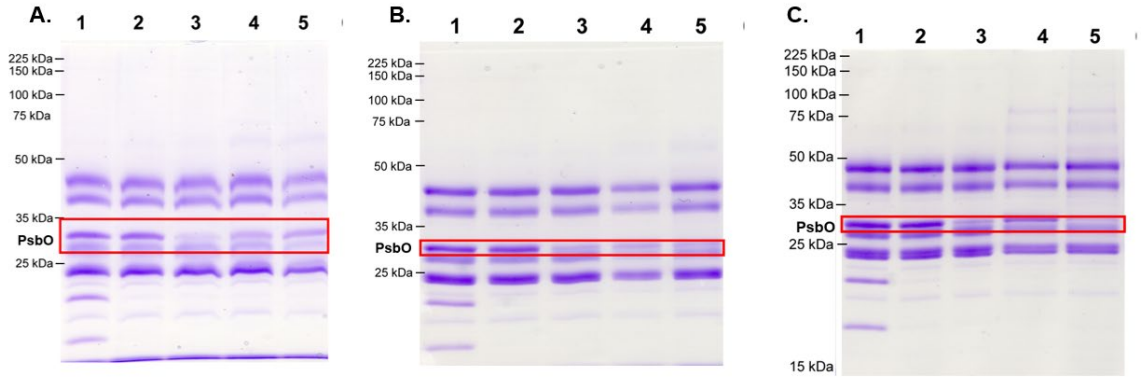

Figure 9 – CNF40(A)/57(B)/155(C)-PsbO-PSII reconstitution SDS-PAGE gel. Lane 1, OTG-PSII; Lane 2, SW-PSII; Lane 3, UW-PSII; Lane 4, WT-PsbO-PSII; Lane 5, CNF40(A)/57(B)/155(C)-PsbO-PSII. PsbO bands are boxed and labelled

Table 3 – Steady-state oxygen evolution activity of CNF40/57/155-PsbO-PSII samples

PSII sample	- Ca^{2+}	+ Ca^{2+}	% SW-PSII
OTG-PSII	1180 ± 50	1240 ± 40	
SW-PSII	660 ± 20	940 ± 20	100%
UW-PSII	390 ± 10	520 ± 10	55%
WT-PsbO-PSII	610 ± 40	790 ± 30	84%
CNF40-PsbO-PSII	580 ± 20	680 ± 40	72%
CNF57-PsbO-PSII	300 ± 20	440 ± 40	47%
CNF155-PsbO-PSII	390 ± 30	520 ± 10	55%

Besides F217 was substituted to CNF217, incorporation at other locations were attempted. The corresponding reconstitution gels (Figure 9) and oxygen evaluation rates (Table 3) are shown above. Lane 5 in each panel is the one got most concern. It was the line of the reconstituted PSII samples. The PsbO bands in lane 5 were faint and thin, which indicated that there were not in a comparable level of PsbO to that in the control bands. It was easy to tell from the oxygen evaluation rates that the reconstitution of CNF40/57/155 neither effectively bound to PSII, nor restored the oxygen evaluation activity as the WT PsbO reconstitution did. In the case, of CNF57, the rate even went lower than that of UW PsbO which was washed off all extrinsic subunits. The problem may come from several sources. First, the DNA sequence of each mutant needs to be double checked to make sure the stop code is at the right place. The DNA sequences were confirmed at the very beginning of the project. However, it is possible that the cell glycerol stab went bad or unexpected mutagenesis occurred in the cell. Second, redo transformation may be necessary. Tetracycline was the antibiotic used as selection for the successful transformation of the pDule-pCNF plasmid. Tetracycline is sensitive to light. Even though

its antibiotic stock solution was stocked at – 20 ℃ and covered by foil, it may degrade during the bacteria growth process which may take more than 24 hours, and as a result, the selection did not really function as expected. pDule2-pCNF can be tested as an alternative. It uses spectinomycin for selection. Spectinomycin is supposed to more stable to survive and function properly during the bacteria growth process.

3.2 Native PsbO, R-V235A PsbO and WT PsbO secondary structure analysis

The CD spectra and secondary structure analysis showed no significant difference among all PsbO samples at all three temperature conditions. (Figure 9) As the temperature increasing, the magnitude around 200 nm significantly increased, which is a characterization of random coils and turns.[130] Based on the secondary structure analysis (Table 4), the heating led to the loss of beta sheet and increase of random turns and coils. The cooling resulted in the recovery of structured region percentage and decrease of the random coils and turns part. Both R-V235A PsbO and WT PsbO showed reversibility, while native PsbO could only reverse part of the change.

Compared with previously published data, the percentage of α helix was comparable to the result here, while the percentage of β sheet and random coils are around 10% off. Less β sheet and more random coils were detected in my case.[84, 131] Besides, R-V235A PsbO and native PsbO were reported to be reversible under this experimental condition.[84, 131] However, native PsbO did not show reversibility, while R-V235A PsbO does. Another conflict is that under same temperature condition, the secondary structure analysis results showed no significant difference among PsbO samples, but the CD spectra of PsbO samples in Figure 10 D-F could not overlap well. Moreover, the data shown here cannot overlap well with the published data collected by other labs.[84, 131]

The CD spectra of CNF PsbO samples will be collected, and their secondary structure will be analyzed. The incorporation of CNF into PsbO is not supposed to cause significant secondary structure change.

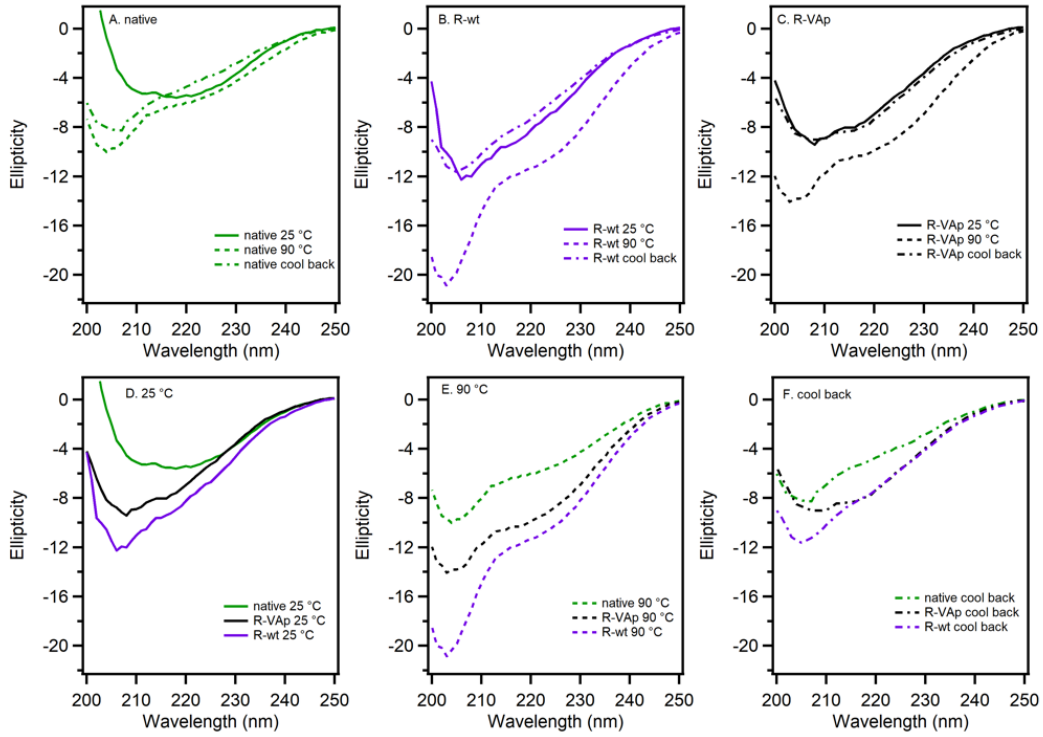

Figure 10 – CD spectra of native PsbO (green), WT PsbO (purple) and R-V235A PsbO (black). Protein samples were in 10 mM KH_2PO_4, pH 6.0. CD spectra were acquired at 25 °C (solid). Each sample was them melted at 90 °C (dashed) in a Peltier cell and subsequently cooled back down to 25 °C (dot-dashed). Panel A, B and C are the melting profile of native PsbO, R-wt PsbO and R-VAp PsbO, respectively. In D-F, comparisons of three types of PsbO are shown at 25 °C (D), 90 °C (E) and 25 °C post-melt (F). Vertical tick marks represent 2 mdeg.

Table 4 – PsbO samples secondary structure composition analysis

	% α-helix	% β-sheet	% turns	% other
Native PsbO 25 ℃	5.5	36.3	58.2	0
Native PsbO post-melt 25 ℃	4.7	34.7	60.6	0
Native PsbO 90 ℃	5.1	30.6	64.3	0
R-V235A PsbO 25 ℃	5.1	35.3	59.6	0
R-V235A PsbO post-melt 25 ℃	6.0	34.0	60.0	0
R-V235A PsbO 90 ℃	5.2	25.5	69.3	0
WT PsbO 25 ℃	7.0	33.1	59.9	0
WT PsbO post-melt 25 ℃	5.8	32.2	62.0	0
WT PsbO 90 ℃	3.6	21.9	74.5	0

3.3 PsbO ultra-violet resonance Raman spectroscopy experimental condition investigation

3.3.1 Optimal laser power and CNF limit of detection

Under multiple laser powers UV irradiation, a gradient of CNF was used to test the limit of detection (LOD) concentration. 20 μM CNF was required to give the 3225 cm^{-1} peak when the laser power was stronger than 1.5 mW. (Figure 10) In general, higher laser power gave UVRR spectra with higher S/N. Increase of sample concentration significantly helped enhance the S/N when the concentration was lower than 20 μM. When the concentration was higher than 20 μM, increasing concentration did not improve the magnitude of signal. 20 μM is the LOD of CNF in the Raman experiment. The UVRR spectrum of 20 μM CNF is optimized under 3.8 mW laser probing. A gradient of laser power was tested. Laser power of 3.8 mW maximized the signal-to-noise ratio (S/N) of the spectrum with no significant UV damage to the sample. (Figure 15) High laser power did

not come with corresponding level of S/N enhancement and there would be higher risk of photodamage on protein sample.

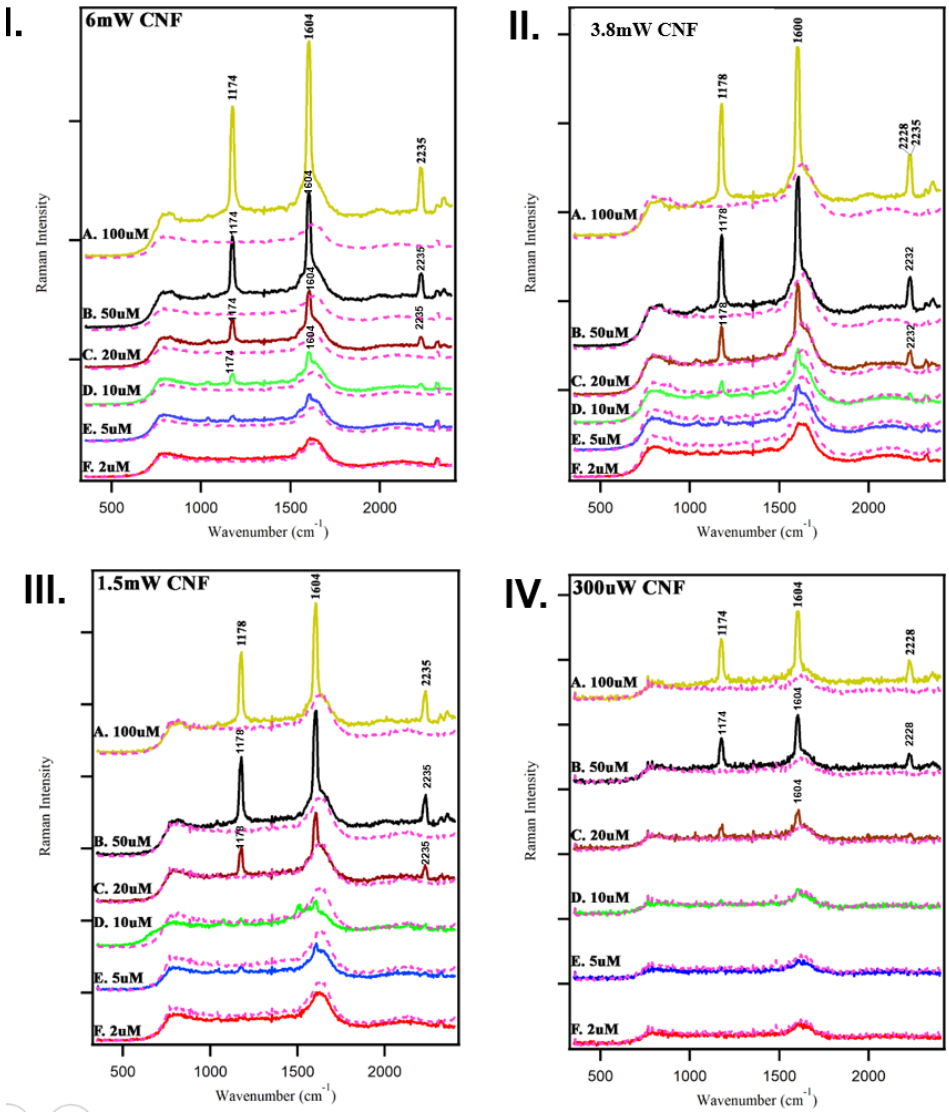

Figure 11 – UVRR spectra of CNF for optimal laser power investigation. In each panel, A-100 µM CNF-yellow-solid line; B-50 µM CNF-black-solid line; C-20 µM CNF-brown-solid line; D-10 µM CNF-green-solid line; E-5 µM CNF-blue-solid line; F-2 µM CNF-red-solid line; all magenta dashed line superimposed with A-F is spectra of buffer. I-IV panel was performed under different laser power. I.-6 mW; II.-3.8 mW; III.-1.5 mW; IV.-300 µW.

3.3.2 PsbO limit of detection

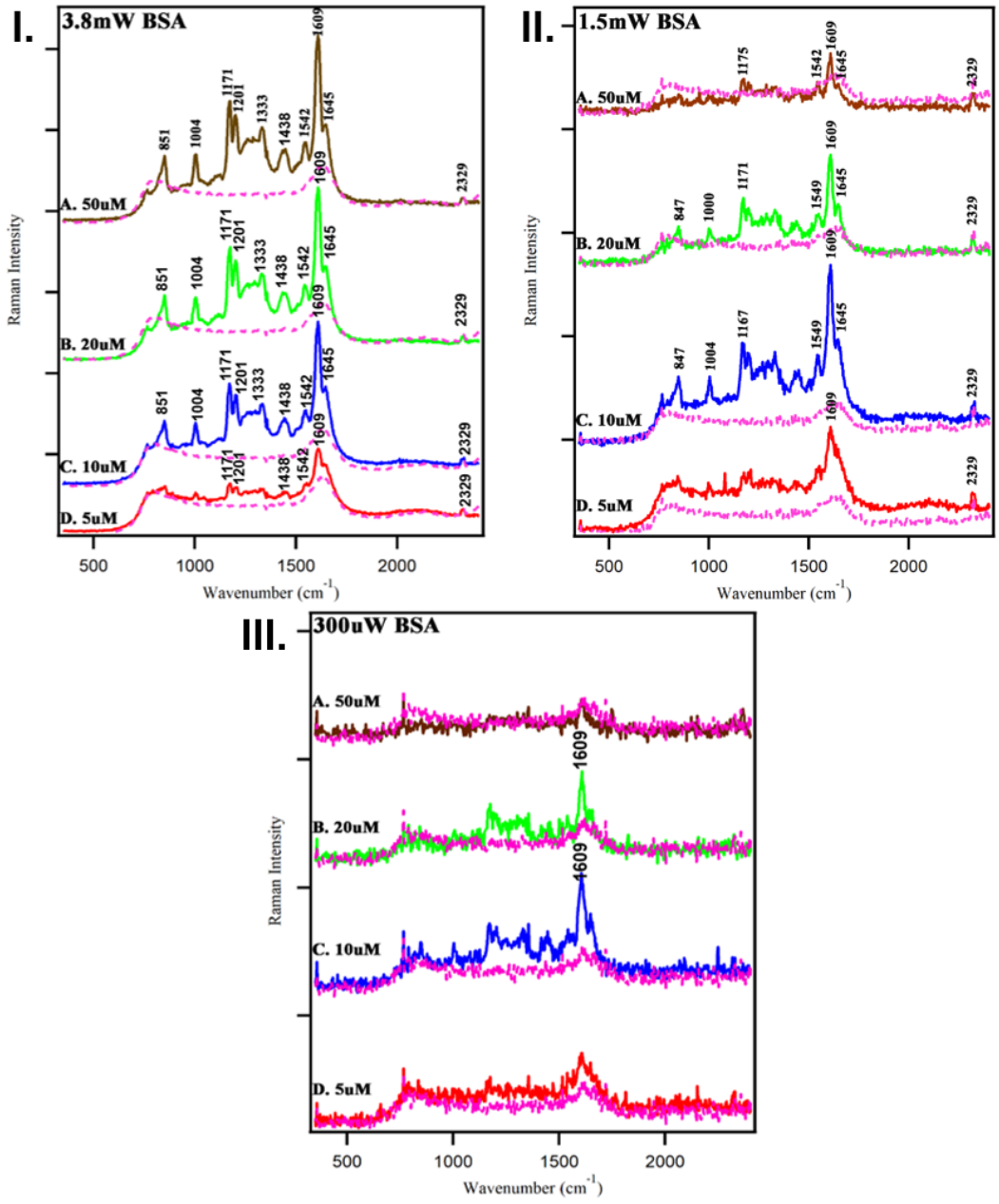

Figure 12 – UVRR spectra of BSA concentration gradient. In each panel, A-50 µM BSA-dark green-solid line; B-20 µM BSA-green-solid line; C-10 µM BSA-blue-solid

line; D-5 μM BSA-red-solid line; all magenta dashed line is spectra of buffer. I-III panel was performed under different laser power with UV probe 244 nm. I.-3.8 mW; II.-1.5 mW; III.-300 μW.

Commercially purchased BSA was used to test the protein limit of detection concentration. Under optimal laser power UV irradiation, 3.8 mW, 10 μM BSA spectrum showed good S/N. (Figure 11) Number of each aromatic amino acid in BSA was more than the double of what in PsbO sequence (Table 5). Therefore, the LOD of PsbO was assumed to be higher than 20 μM.

Table 5 – Number of aromatic amino acid in BSA[132] and PsbO

Aromatic amino acid	BSA (PDB: 4F5S)	PsbO (PDB: 3JCU)
Tyr	20	8
Trp	2	1
Phe	27	13

3.3.3 Single aromatic amino acid UVRR spectra

UVRR spectra of aromatic amino acids (tyrosine, tryptophan, phenylalanine) were collected as controls for the assignment of UVRR bands in PsbO. (Figure 12)

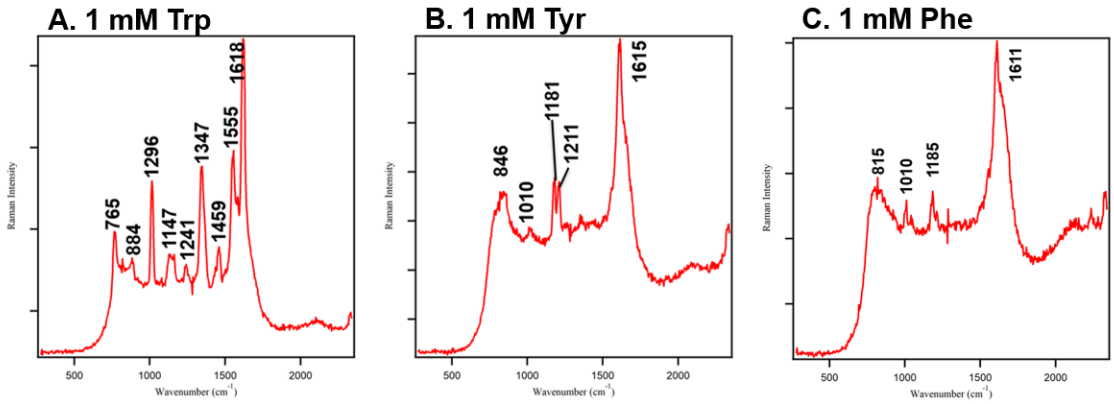

Figure 13 – UVRR spectra of single aromatic amino acid. A-1 mM Trp; B-1 mM Tyr; C-1 mM Phe. Spectra were collected under 3.8 mW UV probe at 244 nm.

3.3.4 45 µM WT PsbO UVRR spectra

20 µM CNF (Figure 13, A) had signature peaks at 1178, 1608 and 2235 cm^{-1}. Two repeats of 20 µM CNF217 PsbO (Figure 13, B and C) could not give UVRR spectra containing protein peaks. Higher concentration of CNF217 PsbO may be required for the detection and optimal of the CN S/N in UVRR spectrum. 45 µM WT PsbO (Figure 13, D) allowed the observation of protein signals. 20 µM 1:1 mixture CNF+WT PsbO (Figure 13, E) showed three signature peaks with good S/N. Meanwhile, the 2235 cm^{-1} peak shifted 7 wavenumber to the hydrophobic direction.

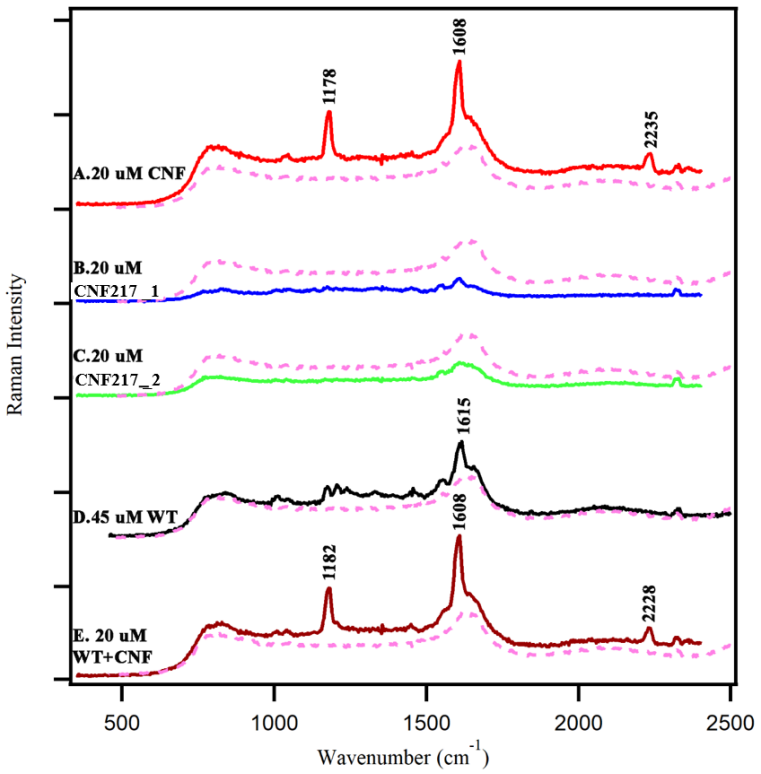

Figure 14 – UVRR spectra of PsbO and controls. A-20 µM CNF-red-solid line; B-20 µM CNF217 PsbO copy 1-blue-solid line; C-20 µM CNF217 PsbO copy 2-green-solid line; D-45 µM WT PsbO-black-solid line; E-20 µM 1:1 mixture of (WT PsbO+CNF)-PsbO-brown-solid line; all magenta dashed line is spectra of buffer. Spectra were collected under 3.8 mW UV probe at 244 nm.

3.3.5 Photodamage test

Photodamage was assessed by comparing UVRR spectra of 45 µM WT-PsbO under two different UV irradiation exposure times. The spectrum of 45 µM WT-PsbO experienced 4 min UV exposure overlapped well with the 8 min trial. No significant changes to the UVRR spectrum as a result of additional UV irradiation were observed. (Figure 14) The spectrum of 45 µM WT-PsbO experienced 4 min UV exposure overlapped well with the 8 min trial. To exclude the possibility that the sample had already been damaged at the starting point of UV exposure, UV-Vis of sample before applied to UVRR experiment and after were collected. No significant change happened to the UV-Vis spectra.

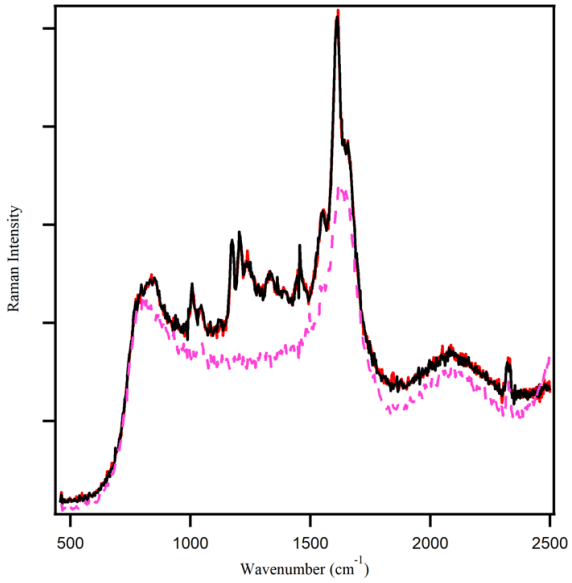

Figure 15 – UVRR spectra for photodamage test. Red solid line, 45 µM WT PsbO exposed to the UV probe for designed experimental condition, 4 min. Black solid line, 45 µM WT PsbO exposed to the same UV probe for double the experiment time, 8 min. Magenta dashed line, spectrum of buffer.

CHAPTER 4. CONCLUSIONS AND DISCUSSIONS

The templating effect of PSII to PsbO has been proposed in published literature. the secondary structure of PsbO undergoes 30-40% change (increase of β-content and decrease of random coils) when bound to PSII.[119] The incorporation of CNF into different locations in PsbO is to identify the residues that may response to the templating impact. The CD data and protein secondary structure study indicated that there is not obvious secondary structure difference among all PsbO samples. The V235A mutation did not make significant effect of the protein structure and melting behavior. CD spectra are designed to make sure there are not significant structural distinction among all types of PsbO. The comparison of UVRR and fluorescence spectra can tell the environmental electrostatic change of each residue before and after bound to PSII.

Since PsbO samples were characterized alone in solution, the templating effect last till PsbO was isolated from PSII. During the reversibility test, native PsbO cannot fully recover its secondary structure which shown as CD spectra could not overlap before and after heating/cooling. This phenomenon may reflect that the templating effect could be broken by exogenous damage (e.g. heating to 90 ℃) and the damage cannot auto-recover by cooling. Other restrictions on the templating effect can be studied in the future.

CNF has been successfully incorporated into PsbO residue 217. Its incorporation maintained the function of PsbO in PSII. The methods and experimental details applied in the process can support the further incorporation of other proposed residue positions, for example, F55, F155 and F57. In addition to the substitution of phenylalanine, other

aromatic amino acid, like tyrosine, can be considered to practice this method to facilitate the probing of protein structural conformation. The influence of nitrile group to the hydrogen bonding map in PsbO could be reflected by the intrinsic fluorescence of PsbO. Experimental conditions investigated to improve the S/N of UVRR spectrum, while preventing the protein sample from photodamage and minimizing the amount of protein sample required in each trial, could benefit future UVRR spectroscopy experiment. Moreover, distinction of UVRR spectra between CNF PsbO samples and templated CNF PsbO samples could provide information on how and where PsbO responds to PSII, thanks to the probing of nitrile group.

Speaking of future direction, the achievement of site-specific incorporation of CNF at 155 may be exciting. F155 was located in the proposed proton exit pathway. UVRR data collection while lasing the CNF155-PsbO-PSII could tell how PsbO made conformational change to function properly and to get involved in the proton exit pathway during the OEC five S-state cycle.

Finally, the work in this thesis provides a method to introduce vibrational probe into PsbO and techniques/experimental details to characterize the conformation of PsbO. These results can benefit future research on PsbO conformation study and help deeper discovery PsbO conformation-function relationship. This is especially meaningful in the case that PsbO is an IDP. The methods and conclusions collected in the process can provide a framework for conformation study of other IDPs that may have essential function in other areas of biochemistry.

REFERENCES

1. Umena, Y.; Kawakami, K.; Shen, J.-R.; Kamiya, N. Crystal Structure of Oxygen-Evolving Photosystem II at a Resolution of 1.9 Angstrom. *Nature* **2011,** *473*, 55-60.

2. Suga, M.; Akita, F.; Hirata, K.; Ueno, G.; Murakami, H.; Nakajima, Y.; Shimizu, T.; Yamashita, K.; Yamamoto, M.; Ago, H., et al. Native Structure of Photosystem II at 1.95 a Resolution Viewed by Femtosecond X-Ray Pulses. *Nature* **2015,** *517*, 99-103.

3. Wei, X.; Su, X.; Cao, P.; Liu, X.; Chang, W.; Li, M.; Zhang, X.; Liu, Z. Structure of Spinach Photosystem II-LHCII Supercomplex at 3.2 Angstrom Resolution. *Nature* **2016,** *534*, 69-74.

4. Nelson, N.; Yocum, C. F. Structure and Function of Photosystems I and II *Ann. Rev. Plant Biol.* **2006,** *57*, 521-565.

5. Barry, B. A. Proton Coupled Electron Transfer and Redox Active Tyrosines in Photosystem II. *J. Photochem. Photobiol. B* **2011,** *104*, 60-71.

6. van Bezouwen, L. S.; Caffarri, S.; Kale, R. S.; Kouril, R.; Thunnissen, A. W. H.; Oostergetel, G. T.; Boekema, E. J. Subunit and Chlorophyll Organization of the Plant Photosystem II Supercomplex. *Nat Plants* **2017,** *3*, 17080-17091.

7. Sheng, X.; Watanabe, A.; Li, A.; Kim, E.; Song, C.; Murata, K.; Song, D.; Minagawa, J.; Liu, Z. Structural Insight into Light Harvesting for Photosystem II in Green Algae. *Nature plants* **2019,** *5*, 1320-1330.

8. Ago, H.; Adachi, H.; Umena, Y.; Tashiro, T.; Kawakami, K.; Kamiya, N.; Tian, L.; Han, G.; Kuang, T.; Liu, Z. Novel Features of Eukaryotic Photosystem II Revealed by Its Crystal Structure Analysis from a Red Alga. *J. Phys. Chem.* **2016,** *291*, 5676-5687.

9. Nagao, R.; Kato, K.; Suzuki, T.; Ifuku, K.; Uchiyama, I.; Kashino, Y.; Dohmae, N.; Akimoto, S.; Shen, J.-R.; Miyazaki, N. Structural Basis for Energy Harvesting and Dissipation in a Diatom PSII–FCPII Supercomplex. *Nature plants* **2019,** *5*, 890-901.

10. Hellmich, J.; Bommer, M.; Burkhardt, A.; Ibrahim, M.; Kern, J.; Meents, A.; Müh, F.; Dobbek, H.; Zouni, A. Native-Like Photosystem II Superstructure at 2.44 Å Resolution through Detergent Extraction from the Protein Crystal. *Structure* **2014,** *22*, 1607-1615.

11. Young, I. D.; Ibrahim, M.; Chatterjee, R.; Gul, S.; Fuller, F. D.; Koroidov, S.; Brewster, A. S.; Tran, R.; Alonso-Mori, R.; Kroll, T., et al. Structure of Photosystem II and Substrate Binding at Room Temperature. *Nature* **2016,** *540*, 453-457.

12. Tanaka, A.; Fukushima, Y.; Kamiya, N. Two Different Structures of the Oxygen-Evolving Complex in the Same Polypeptide Frameworks of Photosystem II. *J. Am. Chem. Soc.* **2017,** *139*, 1718-1721.

13. Suga, M.; Akita, F.; Yamashita, K.; Nakajima, Y.; Ueno, G.; Li, H.; Yamane, T.; Hirata, K.; Umena, Y.; Yonekura, S. An Oxyl/Oxo Mechanism for Oxygen-Oxygen Coupling in PSII Revealed by an X-Ray Free-Electron Laser. *Science* **2019,** *366*, 334-338.

14. Zouni, A.; Witt, H. T.; Kern, J.; Fromme, P.; Krauß, N.; Saenger, W.; Orth, P. Crystal Structure of Photosystem II from *Synechococcus Elongatus* at 3.8 Å Resolution. *Nature* **2001,** *409*, 739-743.

15. Boerner, R. J.; Nguyen, A. P.; Barry, B. A.; Debus, R. J. Evidence from Directed Mutagenesis That Aspartate 170 of the D1 Polypeptide Influences the Assembly and/or Stability of the Manganese Cluster in the Photosynthetic Water-Splitting Complex. *Biochemistry* **1992,** *31*, 6660-6672.

16. Burch, B. D.; Bricker, T. M.; Putnam-Evans, C. Mutations in the Cp43 Protein of Photosystem II Affect Psii Function and Cytochrome C550 Binding. *Atrificial photosynthesis. InTech, Rijeka* **2012**, 53-78.

17. Debus, R. J.; Barry, B. A.; Babcock, G. T.; McIntosh, L. Site-Specific Mutagenesis Identifies a Tyrosine Radical Involved in the Photosynthetic Oxygen-Evolving Complex. *Proc. Nat. Acad. Sci.* **1988,** *85*, 427-430.

18. Zhong, V. Targeted Mutagenesis to Investigate the Role of Low-Molecular-Weight Proteins and a Bicarbonate Cofactor on the Assembly and Function of Photosystem II. University of Otago, 2019.

19. Nickelsen, J.; Rengstl, B. Photosystem II Assembly: From Cyanobacteria to Plants. *Annual review of plant biology* **2013,** *64*, 609-635.

20. Thiel, H.; Varrelmann, M. Identification of a New Psii Target Site Psba Mutation Leading to D1 Amino Acid Leu218Val Exchange in the Chenopodium Album D1 Protein and Comparison to Cross‐Resistance Profiles of Known Modifications at Positions 251 and 264. *Pest management science* **2014,** *70*, 278-285.

21. Boerner, R. J.; Barry, B. A. Isotopic Labeling and Epr Spectroscopy Show That a Tyrosine Residue Is the Terminal Electron Donor, Z, in Manganese-Depleted Photosystem II Preparations. *J. Biol. Chem.* **1993,** *268*, 17151-17154.

22. Brahmachari, U.; Barry, B. A. Dynamics of Proton Transfer to Internal Water During the Photosynthetic Oxygen-Evolving Cycle. *J. Phys. Chem. B* **2016,** *120*, 11464-11473.

23. Brahmachari, U.; Gonthier, J. r. m. F.; Sherrill, C. D.; Barry, B. A. Water Bridges Conduct Sequential Proton Transfer in Photosynthetic Oxygen Evolution. *J. Phys. Chem. B* **2019,** *123*, 4487-4496.

24. Razeghifard, M. R.; Kim, S.; Patzlaff, J. S.; Hutchison, R. S.; Krick, T.; Ayala, I.; Steenhuis, J. J.; Boesch, S. E.; Wheeler, R. A.; Barry, B. A. In Vivo, in Vitro, and

Calculated Vibrational Spectra of Plastoquinone and the Plastosemiquinone Anion Radical. *J. Phys. Chem. B* **1999,** *103*, 9790-9800.

25. Kim, S.; Patzlaff, J.; Krick, T.; Ayala, I.; Sachs, R. K.; Barry, B. A. Isotope-Based Discrimination between the Infrared Modes of Plastosemiquinone Anion Radicals and Neutral Tyrosyl Radicals in Photosystem II. *J. Phys. Chem. B* **2000,** *104*, 9720-9727.

26. Barry, B. A.; Brahmachari, U.; Guo, Z. Tracking Reactive Water and Hydrogen-Bonding Networks in Photosynthetic Oxygen Evolution. *Acc Chem Res* **2017,** *50*, 1937-1945.

27. Shen, J.-R. The Structure of Photosystem II and the Mechanism of Water Oxidation in Photosynthesis. *Annual Review of Plant Biology* **2015,** *66*, 23-48.

28. Dau, H.; Haumann, M. The Manganese Complex of Photosystem II in Its Reaction Cycle—Basic Framework and Possible Realization at the Atomic Level. *Coordination Chemistry Reviews* **2008,** *252*, 273-295.

29. Kok, B.; Forbush, B.; McGloin, M. Cooperation of Charges in Photosynthetic O_2 Evolution–I. A Linear Four Step Mechanism. *Photochem. Photobiol.* **1970,** *11*, 457-475.

30. Kern, J.; Alonso-Mori, R.; Tran, R.; Hattne, J.; Gildea, R. J.; Echols, N.; Glöckner, C.; Hellmich, J.; Laksmono, H.; Sierra, R. G. Simultaneous Femtosecond X-Ray Spectroscopy and Diffraction of Photosystem II at Room Temperature. *Science* **2013,** *340*, 491-495.

31. Kern, J.; Alonso-Mori, R.; Hellmich, J.; Tran, R.; Hattne, J.; Laksmono, H.; Glockner, C.; Echols, N.; Sierra, R. G.; Sellberg, J., et al. Room Temperature Femtosecond X-Ray Diffraction of Photosystem II Microcrystals. *Proc. Natl. Acad. Sci.* **2012,** *109*, 9721-6.

32. Kupitz, C.; Basu, S.; Grotjohann, I.; Fromme, R.; Zatsepin, N. A.; Rendek, K. N.; Hunter, M. S.; Shoeman, R. L.; White, T. A.; Wang, D. Serial Time-Resolved Crystallography of Photosystem II Using a Femtosecond X-Ray Laser. *Nature* **2014,** *513*, 261-265.

33. Kern, J.; Tran, R.; Alonso-Mori, R.; Koroidov, S.; Echols, N.; Hattne, J.; Ibrahim, M.; Gul, S.; Laksmono, H.; Sierra, R. G. Taking Snapshots of Photosynthetic Water Oxidation Using Femtosecond X-Ray Diffraction and Spectroscopy. *Nature communications* **2014,** *5*, 1-11.

34. Suga, M.; Akita, F.; Sugahara, M.; Kubo, M.; Nakajima, Y.; Nakane, T.; Yamashita, K.; Umena, Y.; Nakabayashi, M.; Yamane, T., et al. Light-Induced Structural Changes and the Site of O=O Bond Formation in Psii Caught by Xfel. *Nature* **2017,** *543*, 131-135.

35. Kern, J.; Chatterjee, R.; Young, I. D.; Fuller, F. D.; Lassalle, L.; Ibrahim, M.; Gul, S.; Fransson, T.; Brewster, A. S.; Alonso-Mori, R. Structures of the Intermediates of Kok's Photosynthetic Water Oxidation Clock. *Nature* **2018,** *563*, 421-425.

36. Kulik, L. V.; Epel, B.; Lubitz, W.; Messinger, J. Electronic Structure of the Mn4o X Ca Cluster in the S0 and S2 States of the Oxygen-Evolving Complex of Photosystem II Based on Pulse 55mn-Endor and Epr Spectroscopy. *J. Am. Chem. Soc.* **2007,** *129*, 13421-13435.

37. Robblee, J. H.; Messinger, J.; Cinco, R. M.; McFarlane, K. L.; Fernandez, C.; Pizarro, S. A.; Sauer, K.; Yachandra, V. K. The Mn Cluster in the S_0 State of the Oxygen-Evolving Complex of Photosystem II Studied by Exafs Spectroscopy: Are There Three Di-M-Oxo-Bridged Mn2 Moieties in the Tetranuclear Mn Complex? *J. Am. Chem. Soc.* **2002,** *124*, 7459-7471.

38. Askerka, M.; Vinyard, D. J.; Wang, J.; Brudvig, G. W.; Batista, V. S. Analysis of the Radiation-Damage-Free X-Ray Structure of Photosystem II in Light of Exafs and Qm/Mm Data. *Biochemistry* **2015,** *54*, 1713-1716.

39. Wang, J.; Askerka, M.; Brudvig, G. W.; Batista, V. S. Insights into Photosystem II from Isomorphous Difference Fourier Maps of Femtosecond X-Ray Diffraction Data and Quantum Mechanics/Molecular Mechanics Structural Models. *ACS Energy Lett* **2017,** *2*, 397-407.

40. Kawashima, K.; Takaoka, T.; Kimura, H.; Saito, K.; Ishikita, H. O 2 Evolution and Recovery of the Water-Oxidizing Enzyme. *Nature communications* **2018,** *9*, 1-11.

41. Li, X.; Siegbahn, P. E. Alternative Mechanisms for O 2 Release and O–O Bond Formation in the Oxygen Evolving Complex of Photosystem II. *Physical Chemistry Chemical Physics* **2015,** *17*, 12168-12174.

42. Sproviero, E. M.; Gascon, J. A.; McEvoy, J. P.; Brudvig, G. W.; Batista, V. S. Quantum Mechanics/Molecular Mechanics Study of the Catalytic Cycle of Water Splitting in Photosystem II. *J. Am. Chem. Soc.* **2008,** *130*, 3428-3442.

43. Isobe, H.; Shoji, M.; Shen, J.-R.; Yamaguchi, K. Chemical Equilibrium Models for the S3 State of the Oxygen-Evolving Complex of Photosystem II. *Inorganic chemistry* **2016,** *55*, 502-511.

44. Vincent, J. B.; Christou, G. A Molecular " Double-Pivot" Mechanism for Water Oxidation. *Inorganica Chimica Acta* **1987,** *136*, L41-L43.

45. Cox, N.; Pantazis, D. A.; Lubitz, W. Current Understanding of the Mechanism of Water Oxidation in Photosystem II and Its Relation to Xfel Data. *Annual Review of Biochemistry* **2020,** *89*.

46. Tagore, R.; Chen, H.; Crabtree, R. H.; Brudvig, G. W. Determination of M-Oxo Exchange Rates in Di-M-Oxo Dimanganese Complexes by Electrospray Ionization Mass Spectrometry. *J. Am. Chem. Soc.* **2006,** *128*, 9457-9465.

47. McConnell, I. L.; Grigoryants, V. M.; Scholes, C. P.; Myers, W. K.; Chen, P.-Y.; Whittaker, J. W.; Brudvig, G. W. Epr–Endor Characterization of (17o, 1h, 2h) Water in Manganese Catalase and Its Relevance to the Oxygen-Evolving Complex of Photosystem II. *J. Am. Chem. Soc.* **2012,** *134*, 1504-1512.

48. Lohmiller, T.; Krewald, V.; Sedoud, A.; Rutherford, A. W.; Neese, F.; Lubitz, W.; Pantazis, D. A.; Cox, N. The First State in the Catalytic Cycle of the Water-Oxidizing Enzyme: Identification of a Water-Derived M-Hydroxo Bridge. *J. Am. Chem. Soc.* **2017,** *139*, 14412-14424.

49. Charuvi, D.; Nevo, R.; Kaplan-Ashiri, I.; Shimoni, E.; Reich, Z. Studying the Supramolecular Organization of Photosynthetic Membranes within Freeze-Fractured Leaf Tissues by Cryo-Scanning Electron Microscopy. *J Vis Exp* **2016**, 10.3791/54066.

50. Kawakami, K.; Umena, Y.; Kamiya, N.; Shen, J. R. Structure of the Catalytic, Inorganic Core of Oxygen-Evolving Photosystem Ii at 1.9 Angstrom Resolution. *J Photochem. Photobiol. B* **2011,** *104*, 9-18.

51. De Las Rivas, J.; Barber, J. Analysis of the Structure of the PsbO Protein and Its Implications. *Photosynthesis Research* **2004,** *81*, 329-343.

52. Roose, J. L.; Frankel, L. K.; Mummadisetti, M. P.; Bricker, T. M. The Extrinsic Proteins of Photosystem II: Update. *Planta* **2016,** *243*, 889-908.

53. Zhu, Q.; Yang, Y.; Xiao, Y.; Wang, W.; Kuang, T.; Shen, J.-R.; Han, G. Function of PsbO-Asp158 in Photosystem II: Effects of Mutation of This Residue on the Binding of Psbo and Function of PSII in Thermosynechococcus Vulcanus. *Photosynthesis research* **2020**, 1-12.

54. Burnap, R. L.; Qian, M.; Shen, J.-R.; Inoue, Y.; Sherman, L. A. Role of Disulfide Linkage and Putative Intermolecular Binding Residues in the Stability and Binding of the Extrinsic Manganese-Stabilizing Protein to the Photosystem II Reaction Center. *Biochemistry* **1994,** *33*, 13712-13718.

55. Motoki, A.; Usui, M.; Shimazu, T.; Hirano, M.; Katoh, S. A Domain of the Manganese-Stabilizing Protein from *Synechococcus Elongatus* Involved in Functional Binding to Photosystem II. *J. Biol. Chem.* **2002,** *277*, 14747-14756.

56. Popelkova, H.; Commet, A.; Yocum, C. F. Asp157 Is Required for the Function of Psbo, the Photosystem II Manganese Stabilizing Protein. *Biochemistry* **2009,** *48*, 11920-8.

57. Wyman, A. J.; Popelkova, H.; Yocum, C. F. Site-Directed Mutagenesis of Conserved C-Terminal Tyrosine and Tryptophan Residues of Psbo, the Photosystem II

Manganese-Stabilizing Protein, Alters Its Activity and Fluorescence Properties. *Biochemistry* **2008,** *47*, 6490-8.

58. Popelkova, H.; Betts, S. D.; Lydakis-Symantiris, N.; Im, M. M.; Swenson, E.; Yocum, C. F. Mutagenesis of Basic Residues R151 and R161 in Manganese-Stabilizing Protein of Photosystem II Causes Inefficient Binding of Chloride to the Oxygen-Evolving Complex. *Biochemistry* **2006,** *45*, 3107-3115.

59. Roose, J. L.; Yocum, C. F.; Popelkova, H. Function of Psbo, the Photosystem II Manganese-Stabilizing Protein: Probing the Role of Aspartic Acid 157. *Biochemistry* **2010,** *49*, 6042-51.

60. Sasi, S.; Venkatesh, J.; Daneshi, R. F.; Gururani, M. A. Photosystem II Extrinsic Proteins and Their Putative Role in Abiotic Stress Tolerance in Higher Plants. *Plants* **2018,** *7*, 100.

61. Murakami, R.; Ifuku, K.; Takabayashi, A.; Shikanai, T.; Endo, T.; Sato, F. Functional Dissection of Two *Arabidopsis* PsbO Proteins: PsbO1 and PsbO2. *FEBS Lett.* **2005,** *272*, 2165-75.

62. Murakami, R.; Ifuku, K.; Takabayashi, A.; Shikanai, T.; Endo, T.; Sato, F. Characterization of an *Arabidopsis Thaliana* Mutant with Impaired PsbO, One of Two Genes Encoding Extrinsic 33-kDa Proteins in Photosystem II. *FEBS Lett.* **2002,** *523*, 138-42.

63. Liu, H. J.; Frankel, L. K.; Bricker, T. M. Functional Analysis of Photosystem II in a Psbo-1-Deficient Mutant in *Arabidopsis Thaliana*. *Biochemistry* **2007,** *46*, 7607-7613.

64. Lundin, B.; Nurmi, M.; Rojas-Stuetz, M.; Aro, E. M.; Adamska, I.; Spetea, C. Towards Understanding the Functional Difference between the Two PsbO Isoforms in *Arabidopsis Thaliana*--Insights from Phenotypic Analyses of Psbo Knockout Mutants. *Photosyn. Res.* **2008,** *98*, 405-14.

65. Lundin, B.; Hansson, M.; Schoefs, B.; Vener, A. V.; Spetea, C. The *Arabidopsis* Psbo2 Protein Regulates Dephosphorylation and Turnover of the Photosystem II Reaction Centre D1 Protein. *Plant J.* **2007,** *49*, 528-39.

66. Bricker, T. M.; Frankel, L. K. The Psbo1 Mutant of *Arabidopsis* Cannot Efficiently Use Calcium in Support of Oxygen Evolution by Photosystem II. *J. Biol. Chem.* **2008,** *283*, 29022-7.

67. Offenbacher, A. R.; Polander, B. C.; Barry, B. A. An Intrinsically Disordered Photosystem II Subunit, Psbo, Provides a Structural Template and a Sensor of the Hydrogen-Bonding Network in Photosynthetic Water Oxidation. *J. Biol. Chem.* **2013,** *288*, 29056-68.

68. Popelkova, H.; Yocum, C. F. Psbo, the Manganese-Stabilizing Protein: Analysis of the Structure-Function Relations That Provide Insights into Its Role in Photosystem II. *J. Photochem. Photobiol. B* **2011,** *104*, 179-190.

69. Bricker, T. M.; Roose, J. L.; Fagerlund, R. D.; Frankel, L. K.; Eaton-Rye, J. J. The Extrinsic Proteins of Photosystem II. *Biochim. Biophys. Acta* **2012,** *1817*, 121-42.

70. Yocum, C. F. The Calcium and Chloride Requirements of the O_2 Evolving Complex. *Coord. Chem. Rev.* **2008,** *252*, 296-305.

71. Suzuki, H.; Yu, J.; Kobayashi, T.; Nakanishi, H.; Nixon, P. J.; Noguchi, T. Functional Roles of D2-Lys317 and the Interacting Chloride Ion in the Water Oxidation Reaction of Photosystem II as Revealed by Fourier Transform Infrared Analysis. *Biochemistry* **2013,** *52*, 4748-57.

72. Pokhrel, R.; Service, R. J.; Debus, R. J.; Brudvig, G. W. Mutation of Lysine 317 in the D2 Subunit of Photosystem II Alters Chloride Binding and Proton Transport. *Biochemistry* **2013,** *52*, 4758-73.

73. Xu, Q.; Bricker, T. Structural Organization of Proteins on the Oxidizing Side of Photosystem II. Two Molecules of the 33-kDa Manganese-Stabilizing Proteins Per Reaction Center. *J. Biol. Chem.* **1992,** *267*, 25816-25821.

74. Lorch, S.; Capponi, S.; Pieront, F.; Bondar, A. N. Dynamic Carboxylate/Water Networks on the Surface of the Psbo Subunit of Hoptosystem II. *J. Phys. Chem. B* **2015,** *119*, 12172-81.

75. Debus, R. J. Ftir Studies of Metal Ligands, Networks of Hydrogen Bonds, and Water Molecules near the Active Site Mn(4)Cao(5) Cluster in Photosystem II. *Biochim Biophys Acta* **2015,** *1847*, 19-34.

76. Service, R. J.; Hillier, W.; Debus, R. J. Network of Hydrogen Bonds near the Oxygen-Evolving Mn(4)Cao(5) Cluster of Photosystem II Probed with Ftir Difference Spectroscopy. *Biochemistry* **2014,** *53*, 1001-17.

77. Debus, R. J. Evidence from Ftir Difference Spectroscopy That D1-Asp61 Influences the Water Reactions of the Oxygen-Evolving Mn_4cao_5 Cluster of Photosystem II. *Biochemistry* **2014,** *53*, 2941-55.

78. Nagao, R.; Ueoka-Nakanishi, H.; Noguchi, T. D1-Asn-298 in Photosystem II Is Involved in a Hydrogen-Bond Network near the Redox-Active Tyrosine Yz for Proton Exit During Water Oxidation. *J Biol Chem* **2017**, 10.1074/jbc.M117.815183.

79. Ho, F. M. Structural and Mechanistic Investigations of Photosystem II through Computational Methods. *Biochim. Biophys. Acta* **2012,** *1817*, 106-120.

80. Freier, E.; Wolf, S.; Gerwert, K. Proton Transfer Via a Transient Linear Water-Molecule Chain in a Membrane Protein. *Proc. Natl. Acad. Sci. U.S. A.* **2011,** *108*, 11435-9.

81. Floris, J.; Pim, W.; Djurre, H.; Siewert, J. Molecular Dynamics of Photosystem II Embedded in the Thylakoid Membrane. *Journal of physical chemistry* **2017**.

82. del Val, C.; Bondar, A.-N. Charged Groups at Binding Interfaces of the PsbO Subunit of Photosystem II: A Combined Bioinformatics and Simulation Study. *Biochimica et Biophysica Acta (BBA)-Bioenergetics* **2017,** *1858*, 432-441.

83. Ahmad, M.; Gu, W.; Geyer, T.; Helms, V. Adhesive Water Networks Facilitate Binding of Protein Interfaces. *Nature communications* **2011,** *2*, 1-7.

84. Lydakis-Simantiris, N.; Hutchison, R. S.; Betts, S. D.; Barry, B. A.; Yocum, C. F. Manganese Stabilizing Protein of Photosystem II Is a Thermostable, Natively Unfolded Protein. *Biochemistry* **1999,** *38*, 404-414.

85. Bommer, M.; Bondar, A. N.; Zouni, A.; Dobbek, H.; Dau, H. Crystallographic and Computational Analysis of the Barrel Part of the PsbO Protein of Photosystem II: Carboxylate-Water Clusters as Putative Proton Transfer Relays and Structural Switches. *Biochemistry* **2016,** *55*, 4626-35.

86. Su, X.; Ma, J.; Wei, X.; Cao, P.; Zhu, D.; Chang, W.; Liu, Z.; Zhang, X.; Li, M. Structure and Assembly Mechanism of Plant $C_2S_2M_2$-Type PSII-LHCII Supercomplex. *Science* **2017,** *357*, 815-820.

87. Uversky, V. N.; Dunker, A. K. Understanding Protein Non-Folding. *Biochimica et Biophysica Acta (BBA)-Proteins and Proteomics* **2010,** *1804*, 1231-1264.

88. Wright, P. E.; Dyson, H. J. Intrinsically Disordered Proteins in Cellular Signalling and Regulation. *Nat Rev Mol Cell Biol* **2015,** *16*, 18-29.

89. Xue, B.; Dunbrack, R. L.; Williams, R. W.; Dunker, A. K.; Uversky, V. N. Pondr-Fit: A Meta-Predictor of Intrinsically Disordered Amino Acids. *Biochim Biophys Acta* **2010,** *1804*, 996-1010.

90. Uversky, V. N.; Roman, A.; Oldfield, C. J.; Dunker, A. K. Protein Intrinsic Disorder and Human Papillomaviruses: Increased Amount of Disorder in E6 and E7 Oncoproteins from High Risk Hpvs. *Journal of proteome research* **2006,** *5*, 1829-1842.

91. Trabjerg, E.; Nazari, Z. E.; Rand, K. D. Conformational Analysis of Complex Protein States by Hydrogen/Deuterium Exchange Mass Spectrometry (Hdx-Ms): Challenges and Emerging Solutions. *TrAC Trends in Analytical Chemistry* **2018,** *106*, 125-138.

92. Hébrard, E.; Bessin, Y.; Michon, T.; Longhi, S.; Uversky, V. N.; Delalande, F.; Van Dorsselaer, A.; Romero, P.; Walter, J.; Declerck, N. Intrinsic Disorder in Viral

Proteins Genome-Linked: Experimental and Predictive Analyses. *Virology journal* **2009,** *6*, 23.

93. Popelkova, H.; Wyman, A.; Yocum, C. F. Amino Acid Sequences and Solution Structures of Manganese Stabilizing Protein That Affect Reconstitution of Photosystem II Activity. *Photosyn. Res.* **2003,** *77*, 21-34.

94. Gosavi, P. M.; Korendovych, I. V. Minimalist IR and Fluorescence Probes of Protein Function. *Current opinion in chemical biology* **2016,** *34*, 103-109.

95. Tucker, M. J.; Oyola, R.; Gai, F. A Novel Fluorescent Probe for Protein Binding and Folding Studies: P‐Cyano‐Phenylalanine. *Biopolymers: Original Research on Biomolecules* **2006,** *83*, 571-576.

96. Martin, J. P.; Fetto, N. R.; Tucker, M. J. Comparison of Biological Chromophores: Photophysical Properties of Cyanophenylalanine Derivatives. *Physical Chemistry Chemical Physics* **2016,** *18*, 20750-20757.

97. Fried, S. D.; Boxer, S. G. Measuring Electric Fields and Noncovalent Interactions Using the Vibrational Stark Effect. *Accounts of chemical research* **2015,** *48*, 998-1006.

98. Liu, J.; Strzalka, J.; Tronin, A.; Johansson, J. S.; Blasie, J. K. Mechanism of Interaction between the General Anesthetic Halothane and a Model Ion Channel Protein, Ii: Fluorescence and Vibrational Spectroscopy Using a Cyanophenylalanine Probe. *Biophysical journal* **2009,** *96*, 4176-4187.

99. Adhikary, R.; Zimmermann, J. r.; Dawson, P. E.; Romesberg, F. E. Temperature Dependence of Cn and Scn IR Absorptions Facilitates Their Interpretation and Use as Probes of Proteins. *Analytical chemistry* **2015,** *87*, 11561-11567.

100. Adhikary, R.; Zimmermann, J.; Dawson, P. E.; Romesberg, F. E. IR Probes of Protein Microenvironments: Utility and Potential for Perturbation. *ChemPhysChem* **2014,** *15*, 849-853.

101. Pagba, C. V.; Barry, B. A. Redox-Induced Conformational Switching in Photosystem-II-Inspired Biomimetic Peptides: A Uv Resonance Raman Study. *J. Phys. Chem. B* **2012,** *116*, 10590-10599.

102. Pagba, C. V.; McCaslin, T. G.; Veglia, G.; Porcelli, F.; Yohannan, J.; Guo, Z.; McDaniel, M.; Barry, B. A. A Tyrosine-Tryptophan Dyad and Radical-Based Charge Transfer in a Ribonucleotide Reductase-Inspired Maquette. *Nature Comm.* **2015,** *10010*.

103. Hwang, H.; McCaslin, T. G.; Hazel, A.; Pagba, C. V.; Nevin, C. M.; Pavlova, A.; Barry, B. A.; Gumbart, J. C. Redox-Driven Conformational Dynamics in a Photosystem-Ii-Inspired B-Hairpin Maquette Determined through Spectroscopy and Simulation. *J. Phys. Chem. B* **2017,** *121*, 3536-3545.

104. Wong, C.-Y.; Eftink, M. Biosynthetic Incorporation of Tryptophan Analogues into Staphylococcal Nuclease: Effect of 5-Hydroxytryptophan and 7-Azatryptophan on Structure and Stability. *Protein Sci.* **1997,** *6*, 689-697.

105. Offenbacher, A. R.; Pagba, C. V.; Polander, B. C.; Brahmachari, U.; Barry, B. A. First Site-Specific Incorporation of a Noncanonical Amino Acid into the Photosynthetic Oxygen-Evolving Complex. *ACS Chem Biol* **2014,** *9*, 891-6.

106. Offenbacher, A. R.; Chen, J.; Barry, B. A. Perturbations of Aromatic Amino Acids Are Associated with Iron Cluster Assembly in Ribonucleotide Reductase. *J. Am. Chem. Soc.* **2011,** *133*, 6978-88.

107. Garczarek, F.; Gerwert, K. Functional Waters in Intraprotein Proton Transfer Monitored by FTIR Difference Spectroscopy. *Nature* **2006,** *439*, 109-112.

108. Chen, J.; Barry, B. A. Ultraviolet Resonance Raman Microprobe Spectroscopy of Photosystem II. *Photochem. photobiol.* **2008,** *84*, 815-818.

109. Barry, B. A.; Chen, J.; Keough, J.; Jenson, D. L.; Offenbacher, A. R.; Pagba, C. V. Proton Coupled Electron Transfer and Redox Active Tyrosines: Structure and Function of the Tyrosyl Radicals in Ribonucleotide Reductase and Photosystem II. *J. Phys. Chem. Lett.* **2012,** *3*, 543-554.

110. Chen, J.; Bender, S. L.; Keough, J. M.; Barry, B. A. Tryptophan as a Probe of Photosystem I Electron Transfer Reactions: A UV Resonance Raman Study. *J. Phys. Chem. B Letters* **2009,** *113*, 11367-11370.

111. McCaslin, T. G.; Pagba, C. V.; Yohannan, J.; Barry, B. A. Specific Metallo-Protein Interactions and Antimicrobial Activity in Histatin-5, an Intrinsically Disordered Salivary Peptide. *Scientific reports* **2019,** *9*, 1-14.

112. Buhrke, D.; Hildebrandt, P. Probing Structure and Reaction Dynamics of Proteins Using Time-Resolved Resonance Raman Spectroscopy. *Chemical Reviews* **2019**.

113. Asamoto, D. K.; Kim, J. E., *Lipid-Protein Interactions*, Springer: 2019, pp 327-349.

114. Berthold, D. A.; Babcock, G. T.; Yocum, C. F. A Highly Resolved, Oxygen-Evolving Photosystem Ii Preparation from Spinach Thylakoid Membranes. *FEBS Letters* **1981,** *134*, 231-234.

115. Mishra, R. K.; Ghanotakis, D. F. Selective Extraction of Cp 26 and Cp 29 Proteins without Affecting the Binding of the Extrinsic Proteins (33, 23 and 17 Kda) and the Dcmu Sensitivity of a Photosystem Ii Core Complex. *Photosyn. Res.* **1994,** *42*, 37-42.

116. Bricker, T. M. Oxygen Evolution in the Absence of the 33-Kilodalton Manganese-Stabilizing Protein. *Biochemistry* **1992,** *31*, 4623-4628.

117. Kuwabara, T.; Murata, T.; Miyao, M.; Murata, N. Partial Degradation of the 18-Kda Protein of the Photosynthetic Oxgyen-Evolving Complex: A Study of a Binding Site. *Biochimica et Biophysica Acta* **1986,** *850*, 146-155.

118. Betts, S. D.; Ross, J. R.; Pichersky, E.; Yocum, C. F. Cold-Sensitive Assembly of a Mutant Manganese-Stabilizing Protein Caused by a Val to Ala Replacement. *Biochemistry* **1996,** *35*, 6302-6307.

119. Hutchison, R. S.; Betts, S. D.; Yocum, C. F.; Barry, B. A. Conformational Changes in the Extrinsic Manganese-Stabilizing Protein Can Occur Upon Binding to the Photosystem II Reaction Center: An Isotope Editing and FTIR Study. *Biochemistry* **1998,** *37*, 5643-5653.

120. Betts, S. D.; Hachigian, T. M.; Pichersky, E.; Yocum, C. F. Reconstitution of the Spinach Oxygen-Evolving Complex with Recombinant *Arabidopsis* Manganese-Stabilitzing Protein. *Plant Mol. Biol.* **1994,** *26*, 117-130.

121. Seitchik, J. L.; Peeler, J. C.; Taylor, M. T.; Blackman, M. L.; Rhoads, T. W.; Cooley, R. B.; Refakis, C.; Fox, J. M.; Mehl, R. A. Genetically Encoded Tetrazine Amino Acid Directs Rapid Site-Specific in Vivo Bioorthogonal Ligation with Trans-Cyclooctenes. *J. Am. Chem. Soc.***2012,** *134*, 2898-2901.

122. Peeler, J. C.; Mehl, R. A., *Unnatural Amino Acids*, Springer: 2012, pp 125-134.

123. Piccioni, R.; Bellemare, G.; Chua, N., *Methods in Chloroplast Molecular Biology*, Edelman, H.; Hallick, R. B.; Chua, N.-H., Eds. Elsevier: Amsterdam, 1982, pp 985-1014.

124. Noren, G. H.; Boerner, R. J.; Barry, B. A. Epr Characterization of an Oxygen-Evolving Photosystem Ii Preparation from the Cyanobacterium, *Synechocystis* 6803. *Biochemistry* **1991,** *30*, 3943-3950.

125. Micsonai, A.; Wien, F.; Bulyáki, É.; Kun, J.; Moussong, É.; Lee, Y.-H.; Goto, Y.; Réfrégiers, M.; Kardos, J. Bestsel: A Web Server for Accurate Protein Secondary Structure Prediction and Fold Recognition from the Circular Dichroism Spectra. *Nucleic acids research* **2018,** *46*, W315-W322.

126. Micsonai, A.; Wien, F.; Kernya, L.; Lee, Y.-H.; Goto, Y.; Réfrégiers, M.; Kardos, J. Accurate Secondary Structure Prediction and Fold Recognition for Circular Dichroism Spectroscopy. *Proc. Natl. Acad. Sci.* **2015,** *112*, E3095-E3103.

127. Offenbacher, A. R.; Chen, J.; Barry, B. A. Perturbations of Aromatic Amino Acids Are Associated with Iron Cluster Assembly in Ribonucleotide Reductase. *J. Am. Chem. Soc.* **2011,** *133*, 6978-6988.

128. Geng, J.; Aioub, M.; El-Sayed, M. A.; Barry, B. A. An Ultraviolet Resonance Raman Spectroscopic Study of Cisplatin and Transplatin Interactions with Genomic DNA. *J. Phys. Chem. B* **2017,** *121*, 8975-8983.

129. Shutova, T.; Deikus, G.; Irrgang, K.-D.; Klimov, V. V.; Renger, G. Origin and Properties of Fluorescence Emission from the Extrinsic 33 Kda Manganese Stabilizing Protein of Higher Plant Water Oxidizing Complex. *Biochimica et Biophysica Acta (BBA)-Bioenergetics* **2001,** *1504*, 371-378.

130. Corrêa, D. H.; Ramos, C. H. The Use of Circular Dichroism Spectroscopy to Study Protein Folding, Form and Function. *Afr. J. Biochem, Res.* **2009,** *3*, 164-173.

131. Wyman, A. J.; Yocum, C. F. Structure and Activity of the Photosystem II Manganese-Stabilizing Protein: Role of the Conserved Disulfide Bond. *Photosynth. Res.* **2005,** *85*, 359-372.

132. Bujacz, A. Structures of Bovine, Equine and Leporine Serum Albumin. *Acta Crystallographica Section D: Biological Crystallography* **2012,** *68*, 1278-1289.